

AD-A228 534

2

OFFICE OF NAVAL RESEARCH  
Contract N00014-89-J-1052  
R & J Code 4134036  
Technical Report No. 51

DTIC FILE COPY

A COMPARATIVE STUDY OF THE CHEMISORPTION OF ETHYLENE  
ON THREE METAL SURFACES: Ni(111), Pd(111) and Pt(111)

by

Yat-Ting Wong and Roald Hoffmann  
Department of Chemistry and Materials Science Center  
Cornell University  
Ithaca, NY 14853 USA

Prepared for Publication  
in  
J. Chem. Soc. Far. Trans.

DTIC  
ELECTE  
OCT 31 1990  
S B D  
Co

Reproduction in whole or in part is permitted  
for any purpose of the United States Government

This document has been approved for public release  
and sale; its distribution is unlimited

**REPORT DOCUMENTATION PAGE**

1a. REPORT SECURITY CLASSIFICATION <b>Unclassified</b>		1b. RESTRICTIVE MARKINGS	
2a. SECURITY CLASSIFICATION AUTHORITY		3. DISTRIBUTION / AVAILABILITY OF REPORT	
2b. DECLASSIFICATION / DOWNGRADING SCHEDULE			
4. PERFORMING ORGANIZATION REPORT NUMBER(S) #51		5. MONITORING ORGANIZATION REPORT NUMBER(S)	
6a. NAME OF PERFORMING ORGANIZATION Department of Chemistry	6b. OFFICE SYMBOL (if applicable)	7a. NAME OF MONITORING ORGANIZATION ONR	
6c. ADDRESS (City, State, and ZIP Code) Cornell University Baker Laboratory Ithaca, NY 14853-1301		7b. ADDRESS (City, State, and ZIP Code) 800 Quincy Street, Arlington, VA	
8a. NAME OF FUNDING / SPONSORING ORGANIZATION Office of Naval Research	8b. OFFICE SYMBOL (if applicable)	9. PROCUREMENT INSTRUMENT IDENTIFICATION NUMBER Report #51	
8c. ADDRESS (City, State, and ZIP Code)		10. SOURCE OF FUNDING NUMBERS	
		PROGRAM ELEMENT NO	PROJECT NO
		TASK NO	WORK UNIT ACCESSION NO
11. TITLE (Include Security Classification) A Comparative Study of the Chemisorption of Ethylene on Three Metal Surfaces: Ni(111), Pd(111) and Pt(111)			
12. PERSONAL AUTHOR(S) Y.-T. Wong and R. Hoffmann			
13a. TYPE OF REPORT Technical Report #51	13b. TIME COVERED FROM _____ TO _____	14. DATE OF REPORT (Year, Month, Day) October 12, 1990	15. PAGE COUNT
16. SUPPLEMENTARY NOTATION			
17. COSATI CODES		18. SUBJECT TERMS (Continue on reverse if necessary and identify by block number)	
FIELD	GROUP	Chemisorption, Ethylene, Ni, Pt, Pd Surfaces	
	SUB-GROUP		
19. ABSTRACT (Continue on reverse if necessary and identify by block number) The chemisorption of ethylene on three metal surfaces, Ni(111), Pd(111) and Pt(111), has been studied by an approximate molecular orbital method: extended Hückel calculations within a tight-binding formalism. The overlap population between individual fragment molecular orbital (FMO) of the adsorbate and each atomic orbital (AO) or atom of the surface can be projected out accurately. The relative importance of each FMO to the ethylene-metal bonding can then be assessed. Moreover, interaction diagrams can be constructed to describe the adsorbate-surface bonding. The preferred adsorption sites determined by our calculations are supported by the vibrational data obtained by electron energy loss scattering. The activation energy for the transformation of a $\pi$ -bonded ethylene to a di- $\sigma$ -bonded adsorbate on Pt(111) has been estimated.			
20. DISTRIBUTION / AVAILABILITY OF ABSTRACT <input checked="" type="checkbox"/> UNCLASSIFIED/UNLIMITED <input type="checkbox"/> SAME AS RPT. <input type="checkbox"/> DTIC USERS		21. ABSTRACT SECURITY CLASSIFICATION unclassified	
22a. NAME OF RESPONSIBLE INDIVIDUAL Roald Hoffmann		22b. TELEPHONE (Include Area Code) 607-255-3419	22c. OFFICE SYMBOL

**A comparative study of the chemisorption of ethylene  
on three metal surfaces: Ni(111), Pd(111) and Pt(111).**

Yat-Ting Wong and Roald Hoffmann\*

*Department of Chemistry and Materials Science Center  
Cornell University, Ithaca, NY 14853, USA.*

**Abstract:** The chemisorption of ethylene on three metal surfaces, Ni(111), Pd(111) and Pt(111), has been studied by an approximate molecular orbital method: extended Hückel calculations within a tight-binding formalism. The overlap population between individual fragment molecular orbital (FMO) of the adsorbate and each atomic orbital (AO) or atom of the surface can be projected out accurately. The relative importance of each FMO to the ethylene-metal bonding can then be assessed. Moreover, interaction diagrams can be constructed to describe the adsorbate-surface bonding. The preferred adsorption sites determined by our calculations are supported by the vibrational data obtained by electron energy loss scattering. The activation energy for the transformation of a  $\pi$ -bonded ethylene to a di- $\sigma$ -bonded adsorbate on Pt(111) has been estimated.

## Introduction

Heterogeneous catalysis on metal surfaces implies enhanced reactivity. Facilitation of a reaction may occur in any of the many steps of a surface mechanism — chemisorption, reaction, migration on the surface, further reaction, desorption. If we are to understand these reactions, we have to understand them in detail for one metal, and, most importantly, how they vary as we pass from one metal to another.

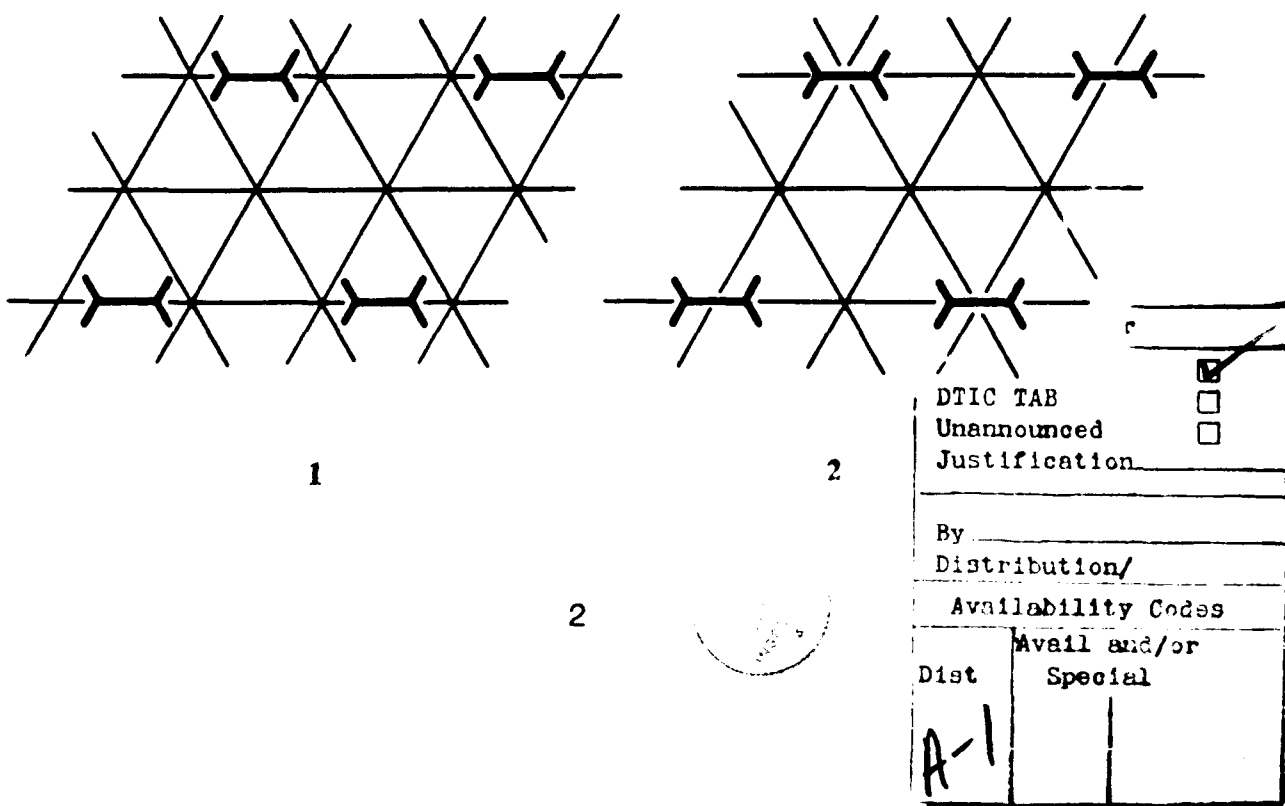
The common crystal forms of the group 10 elements Ni, Pd and Pt are face-centered cubic. The easy-to-come by hexagonal (111) face is a close-packed plane, likely to be minimally reconstructed. For a given adsorbate, we might expect a smooth, gradual change in adsorbate-surface interaction as we go from Ni(111) → Pd(111) → Pt(111). Consider now specifically ethylene. Electron energy loss scattering (EELS) showed that ethylene is more strongly bound and more distorted on Ni(111) and Pt(111) than Pd(111).<sup>1</sup> Comparison of the vibrational spectra also suggested a different adsorption site on Pd(111).<sup>2</sup> This is inconsistent with the simple idea of a gradual change and poses a puzzle.

In this paper, we investigate the chemisorption of ethylene on the above-mentioned three metal surfaces. The tight-binding extended Hückel method is employed to trace down the orbital interactions.<sup>3</sup> As a compromise between accuracy and economy, three-layer slabs serve as models for the metal surfaces. The adsorbate molecules are put on one side of the two-dimensional metal slabs only. This covered layer will be referred to hereafter as the surface layer.

Let us first review the experimental data in some detail, for these have been subjected to some ambiguity and controversy. Ethylene adsorbs initially in a disordered way on Pt(111). After exposure to the electron beam (and probably some decomposition) a (2x2) low energy electron diffraction (LEED) pattern can be observed, indicating a possible coverage,  $\theta$ , of 0.25.<sup>4</sup> This value of  $\theta$  was supported by thermal desorption spectroscopy<sup>5</sup> and radiotracer data,<sup>6</sup> but disagreed with results from X-ray photoelectron

spectroscopy<sup>7,8</sup> and elastic recoil detection.<sup>9</sup> The latter two methods favored  $\theta = 0.5$ . Our calculations will show that for one-half coverage there are extremely large adsorbate-adsorbate repulsions, unless the ethylene molecules are tilted with respect to the surface. This upright position has been detected only on the Pt(111) surface near 300 K, at which temperature decomposition occurred.<sup>10</sup> We wish to concentrate here on low temperature adsorption where the C-C bond is parallel to the surface. So one-quarter coverage seems to be more reasonable. A (2x2) LEED pattern has been obtained for ethylene on Ni(111) as well.<sup>11</sup> The Pt-Pt bond length (2.77 Å) is only slightly longer than that of Pd-Pd (2.75 Å). We thus assume the same coverage,  $\theta = 1/4$ , for all three metal surfaces.

Although the exact geometry and location of the chemisorbed ethylene are unknown, some useful information is available. EELS performed near 100 K pointed to a 2-fold bridge site (di- $\sigma$ -bonded ethylene) **1** for Ni(111) and Pt(111) but an on-top site ( $\pi$ -bonded ethylene) **2** for Pd(111).<sup>2,12-15</sup> The assignment of adsorption site for Ni(111) was supported by near edge extended X-ray absorption fine structure (NEXAFS).<sup>16</sup> This technique, however, favored a  $\pi$ -bonded adsorbate on Pt(111).<sup>10</sup> Adding to this controversy are the recent results of ultra-violet photoelectron spectroscopy (UPS) which suggested the existence of a  $\pi$ -bonded species at temperatures lower than 52 K on Pt(111).



At a temperature higher than 52 K, the adsorbate transforms into a di- $\sigma$ -bonded ethylene.<sup>17</sup> Finally, it is interesting to note that the di- $\sigma$ -bonded ethylene was proposed to be the intermediate for catalytic exchange between ethane and deuterium (the  $\alpha\beta$  process) over evaporated film of Ni, Pd and Pt in the fifties and sixties. More recently the involvement of a  $\pi$ -bonded alkene has been put forward.<sup>18,19</sup> By adjusting the geometry of the ethylene to fit the photoemission results, Demuth suggested a C-C bond length in ethylene of 1.39, 1.44 and 1.49 Å on Ni(111), Pd(111) and Pt(111) respectively,<sup>20</sup> (compared to 1.37 Å in Zeise's salt) and some bending of hydrogen away from the surfaces. The C-C bond length on Pt(111) is in excellent agreement with the NEXAFS data ( $1.49 \pm 0.03$  Å).<sup>21</sup> Room temperature adsorption of ethylene on Ni(111) produced a C<sub>2</sub> surface species with a C-C bond about 1.45 Å.<sup>16</sup> Recent studies on Cu(100) led to a C-C bond lengthening of about 0.13 Å.<sup>22,23</sup>

To simplify the problem within our computational ability, all the C-C bonds, the C-H bonds and the HCH angles of ethylene on Ni(111), Pd(111) and Pt(111) are set to 1.45 Å, 1.10 Å and 120° respectively. The Ni-Ni, Pd-Pd and Pt-Pt bond lengths are kept fixed at 2.49, 2.75 and 2.77 Å. No surface reconstruction or relaxation is presumed. From the known structures of organometallic compounds and the theoretical work of Anderson,<sup>24-27</sup> we assume a metal-carbon bond length of 2.02 Å for ethylene on Ni(111) and 2.10 Å on Pd(111) and Pt(111).

The degree of bending of the hydrogens should be different for each metal surface. The bending angles of the HCH planes with respect to the metal surfaces ( $\phi$ , as defined in 3), were determined by minimizing the total energy. Table 1 displays the optimized bending angles. Despite our drastic approximations, for a given adsorption site ethylene seems to prefer a less distorted geometry on Pd(111), in agreement with the experimental result.

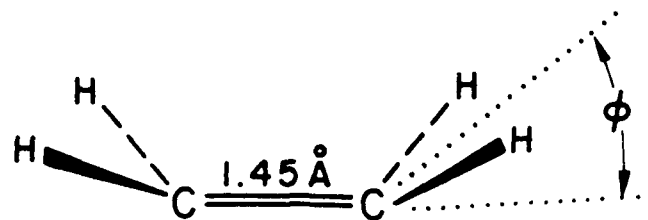
---

Table 1 here

---

Table 1. Optimized HCH Bending Angles ( $\phi$ , see 3) of Ethylene with the Metal Surfaces.

metal surface	2-fold site	atop site
Ni(111)	40°	30°
Pd(111)	25°	15°
Pt(111)	39°	25°



3

Before we proceed to a detailed analysis of the adsorbate-surface interaction, a few words are in order about the two important conceptual tools we use: the density of states (DOS) and its partitions, and the crystal orbital overlap population (COOP) curve. The DOS curve is a graph of the number of orbitals per unit volume per unit energy as abscissa, versus energy as ordinate. That DOS may be partitioned on an atom, atomic orbital, or fragment molecular orbital basis. The COOP curve is a plot of the overlap-population-weighted density of states versus energy. Integration of the COOP curve up to the Fermi energy then gives the total overlap population.<sup>3</sup> Further computational details can be conveniently found in the Appendix.

4

## Comparison of the adsorption of ethylene on Ni(111), Pd(111) and Pt(111)

One of the drawbacks of the non-self-consistent extended Hückel method is the exaggeration of electron transfer. The valence state ionization potentials ( $H_{ii}$ ) for the metals are thus refined by charge iteration of the three-layer slabs with ethylene at the 2-fold site and the on-top site until self-consistency in the metal charge distribution is attained. In this way, the excessive electron flow is greatly reduced. Table 2 gives the  $H_{ii}$ 's of the s, p and d orbitals of Ni, Pd and Pt so obtained. Among the three metals, the energy difference between the d orbitals and the s or p is greatest for palladium. As we shall see later, this leads to some interesting bonding features. Note that the two set of charge self-consistent parameters are not that different.

It is instructive to compare our computed results with those obtained by other theoretical methods. Relativistic augmented-plane-wave calculations suggest that the palladium d band is lower than that of the platinum.<sup>28</sup> This computational technique also indicates that compared to palladium, the platinum sp bands move toward lower energies relative to the d band. There is thus stronger sp-d hybridization in the case of platinum.

---

Table 2 here

---

Calculations have been performed with both sets of parameters (those derived from the on-top and 2-fold site iterations). Selected results for the "2-fold site parameters" are listed in Table 3, those for the "on-top site parameters" in Table 4. The binding energy is defined as the difference in energy between the adsorbate-surface composite system when the planar, undistorted ethylene molecule is removed from the surface and when it is chemisorbed with the above specified geometry. A positive binding energy means an attractive interaction. It seems that on Ni(111) and Pt(111) there is a slight preference for the 2-fold site over the on-top site. The reverse is true on Pd(111). Comparing the binding

Table 2. Valence State Ionization Potentials (in eV) Obtained by Charge Iteration with the Ethylene at the 2-fold or Atop site.

metal surface	2-fold site			atop site		
	s	p	d	s	p	d
Ni(111)	-7.92	-4.18	-11.51	-7.79	-4.08	-11.30
Pd(111)	-7.51	-3.86	-12.53	-7.50	-3.85	-12.51
Pt(111)	-8.82	-5.28	-12.15	-8.75	-5.23	-12.04

energy at the 2-fold site of Ni(111) and Pt(111) with that at the on-top site of Pd(111) suggests that chemisorption on the latter may be weaker. The adsorption of ethylene on Pt(111) occurs even at 37 K.<sup>17</sup> The activation energy for adsorption should be vanishingly small. The activation energy for desorption would then be a good upper bound for the binding energy. The activation energy for desorption of the di- $\sigma$ -bonded and the  $\pi$ -bonded ethylene on Pt(111) are determined experimentally to be 0.39-0.74 and 0.22-0.39 eV, respectively.<sup>29,30</sup> The computed binding energies for ethylene on Pt(111) are probably of the right order of magnitude.

The C-C overlap population (OP) of ethylene and ethane at their equilibrium geometries are 1.300 and 0.737, respectively. Hence the computed overlap populations point to a bond order around 1.5. The C-C OP for the more stable adsorption site on Ni(111), Pt(111) and Pd(111) is calculated to be 0.902, 0.914 and 1.066, respectively (using the 2-fold site parameters). The C-C stretching frequencies for ethylene on Ni(111), Pt(111) and Pd(111) appear to be 1045, 1110 and 1355  $\text{cm}^{-1}$ , respectively,<sup>31</sup> the first two values being the mean values from the surface species derived from  $\text{C}_2\text{H}_4$  and  $\text{C}_2\text{D}_4$ , and the third from the  $\text{C}_2\text{D}_4$  species alone because the  $\text{C}_2\text{H}_4$  spectrum (like that of Zeise's salt and of ethylene itself) is complicated by strong coupling between C-C stretching and  $\text{CH}_2$  scissors modes.<sup>32</sup> An alternate assignment is 1200, 1230 and 1502  $\text{cm}^{-1}$ .<sup>1,14</sup> Zeise's salt ( $\text{KPtCl}_3(\text{CH}_2=\text{CH}_2)$ ) and free ethylene in gas phase values are 1515 and 1623  $\text{cm}^{-1}$ , respectively.

The agreement between the computed results and experiment is reasonable and the trend is not very parameter-sensitive either (compare Table 3 and 4). Similar qualitative features are obtained with either set of parameters, except that the  $H_{ii}$ 's for the on-top site generally give a slightly higher binding energy. Hereafter our discussion will be based on the results derived from the 2-fold site parameters.

---

Table 3 and 4 here

---

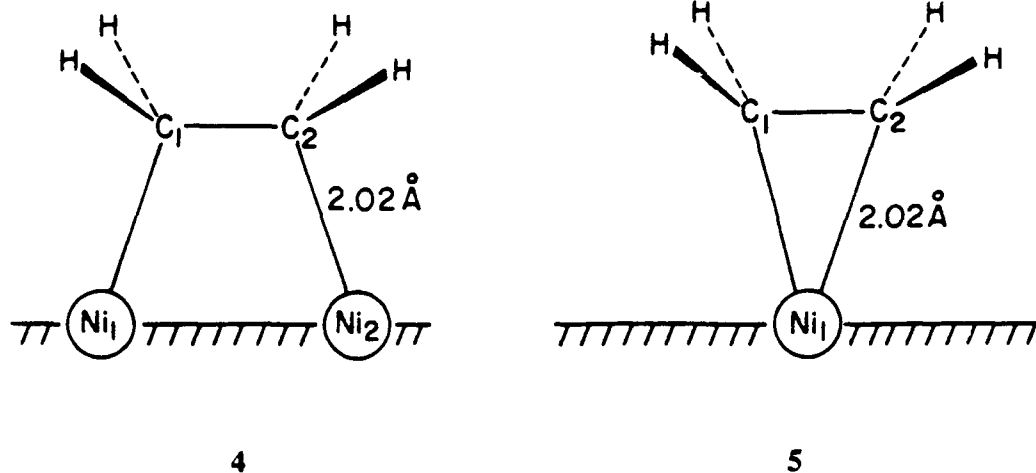
Table 3. Binding Energies and C-C Overlap Populations Calculated with the 2-fold Site Parameters.

metal surface	2-fold site		atop site	
	binding energy (eV)	C-C overlap population	binding energy (eV)	C-C overlap population
Ni(111)	+0.404	0.902	-0.172	0.968
Pd(111)	+0.229	1.040	+0.313	1.066
Pt(111)	+0.583	0.914	+0.401	0.972

Table 4. Binding Energies and C-C Overlap Populations Calculated with the Atop Site Parameters.

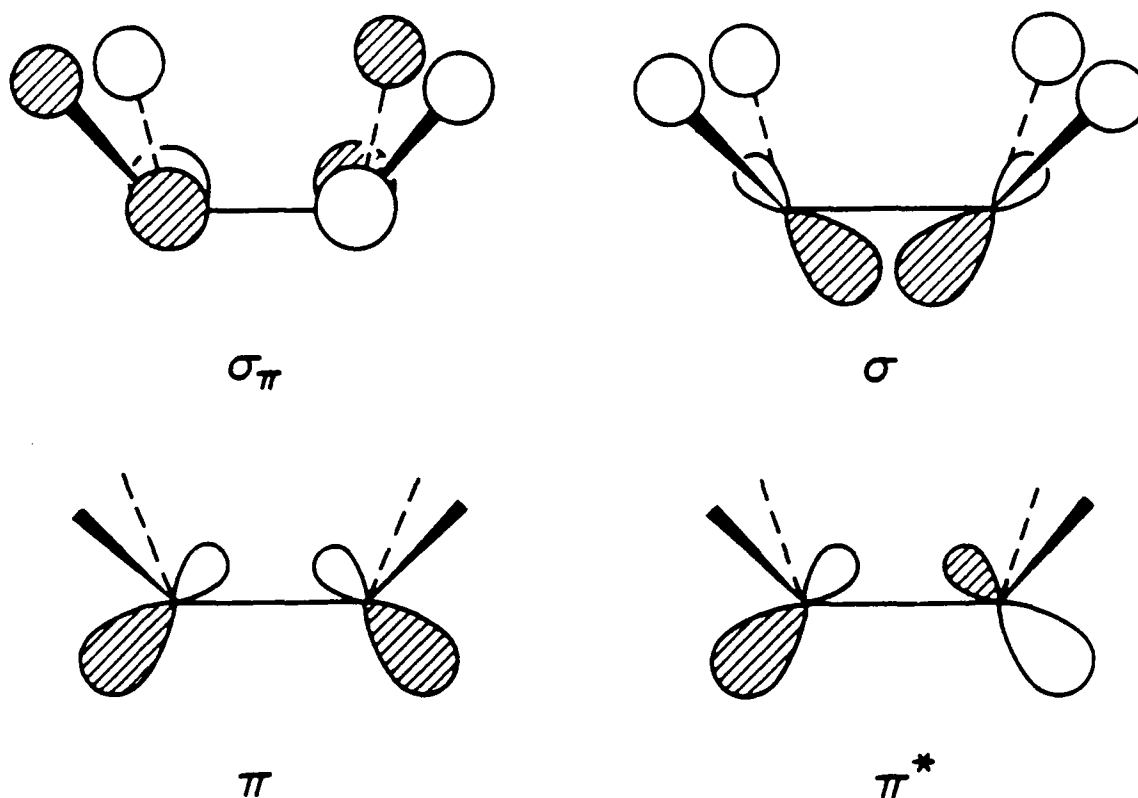
metal surface	2-fold site		atop site	
	binding energy (eV)	C-C overlap population	binding energy (eV)	C-C overlap population
Ni(111)	+0.476	0.894	-0.147	0.962
Pd(111)	+0.232	1.040	+0.316	1.066
Pt(111)	+0.614	0.910	+0.446	0.971

The numbering of atoms at the two adsorption sites of Ni(111) is depicted in 4 and 5. Since (2x2) unit cells have been chosen (see 1 and 2), there is always a mirror



plane bisecting and perpendicular to the C-C bond. Hence, in every adsorption site there are two symmetry-equivalent C-Ni bonds: the Ni<sub>1</sub>-C<sub>1</sub> and Ni<sub>2</sub>-C<sub>2</sub> bond at the 2-fold site; the Ni<sub>1</sub>-C<sub>1</sub> and Ni<sub>1</sub>-C<sub>2</sub> bond at the on-top site. To compare the bonding between 4 and 5, it is sufficient to single out one of the two C-Ni bonds. Hereafter, whenever we refer to the COOP curve or overlap population of a C-Ni bond, we imply the Ni<sub>1</sub>-C<sub>1</sub> bond, be it at the on-top site or the 2-fold site (unless otherwise specified). For compactness, the 2-fold site and on-top site on Ni(111) are abbreviated as Ni(2-fold) and Ni(on-top) respectively. The same conventions apply to the other two surfaces.

From the experience of organometallic chemistry, and the supporting theoretical framework of perturbation theory, we know that the interactions between the central metal atom and its ligands occur mainly through the frontier orbitals. The frontier orbitals of a bent ethylene are, in order of increasing energy,  $\sigma_\pi$ ,  $\sigma$ ,  $\pi$ , and  $\pi^*$  6, the first three of these being fully occupied in neutral ethylene. ( $\sigma_\pi$  is C-H sigma-bonding and C-C pi-antibonding. This is the inspiration for our nomenclature.) We expect them to play an



6

important role on the adsorbate-surface interaction. As we shall see later, for the on-top site on Pd(111) and the 2-fold site on Ni(111) and Pt(111), these orbitals are responsible for 125%, 99% and 98%, respectively of the carbon-metal OP. (The contribution on Pd(111) is greater than 100% because all the other eight orbitals of ethylene produce a net antibonding OP of -0.041.) Thus, the following analysis will concentrate on these four frontier orbitals.

Figure 1 is the analogue of an interaction diagram in molecular chemistry. In the left panel is the total density of states (DOS) of a monolayer of ethylene arranged in the same geometry as the adsorbed layer at the 2-fold site of Ni(111). The  $\pi$  and  $\pi^*$  band then correspond to the highest occupied molecular orbital (HOMO) and the lowest unoccupied molecular orbital (LUMO) of a discrete molecule. There is extensive overlapping of the

8

DOS of  $\sigma$  and  $\sigma_\pi$  near -15 eV. Judging from the narrowness of the bands, the adsorbate-adsorbate interaction at one-quarter coverage is small. This is expected, for the closest H...H contact between neighboring ethylene molecules at this coverage is 2.42 Å. Energetically, this steric interaction costs only about 0.049 eV.

---

Figure 1 here

---

The right panel is the DOS of the bare Ni(111) surface. The position of the Fermi energy suggests that most of the d bands are filled. Indeed, for the surface atoms of bare Ni(111), Pd(111) and Pt(111), the computed electronic configurations are  $d^{9.47}s^{0.40}p^{0.18}$ ,  $d^{9.81}s^{0.10}p^{0.09}$  and  $d^{9.36}s^{0.46}p^{0.23}$ , respectively. The electron occupation of the valence s orbitals seems to be slightly lower, that of the p slightly greater than would have been anticipated. The width of the d bands is about 4 eV, while the dispersions of the s and p bands are much larger, reflecting the much more contracted nature of the d orbitals.

In the middle panel, we display the total density of states of ethylene (shaded) after adsorption. In reality, the Fermi energy of the metal surfaces should not move after adsorption. It does so in our calculations, because of the finite thickness of the slabs. The shifts, however, are very small ( in this work always less than 0.13 eV).

The projected DOS of the four important frontier orbitals, magnified by a factor of five, is displayed in Figure 2. The horizontal "sticks" display the positions of the MO's in a free, planar, undistorted ethylene molecule. After adsorption, about 18% of the DOS of  $\pi$  is pushed up above the Fermi energy and the main body of this band is pushed down by approximately 0.5 eV. From the integration curve, about 44% of the  $\pi^*$  gets occupied. It also develops substantial dispersion, indicative of strong interaction.

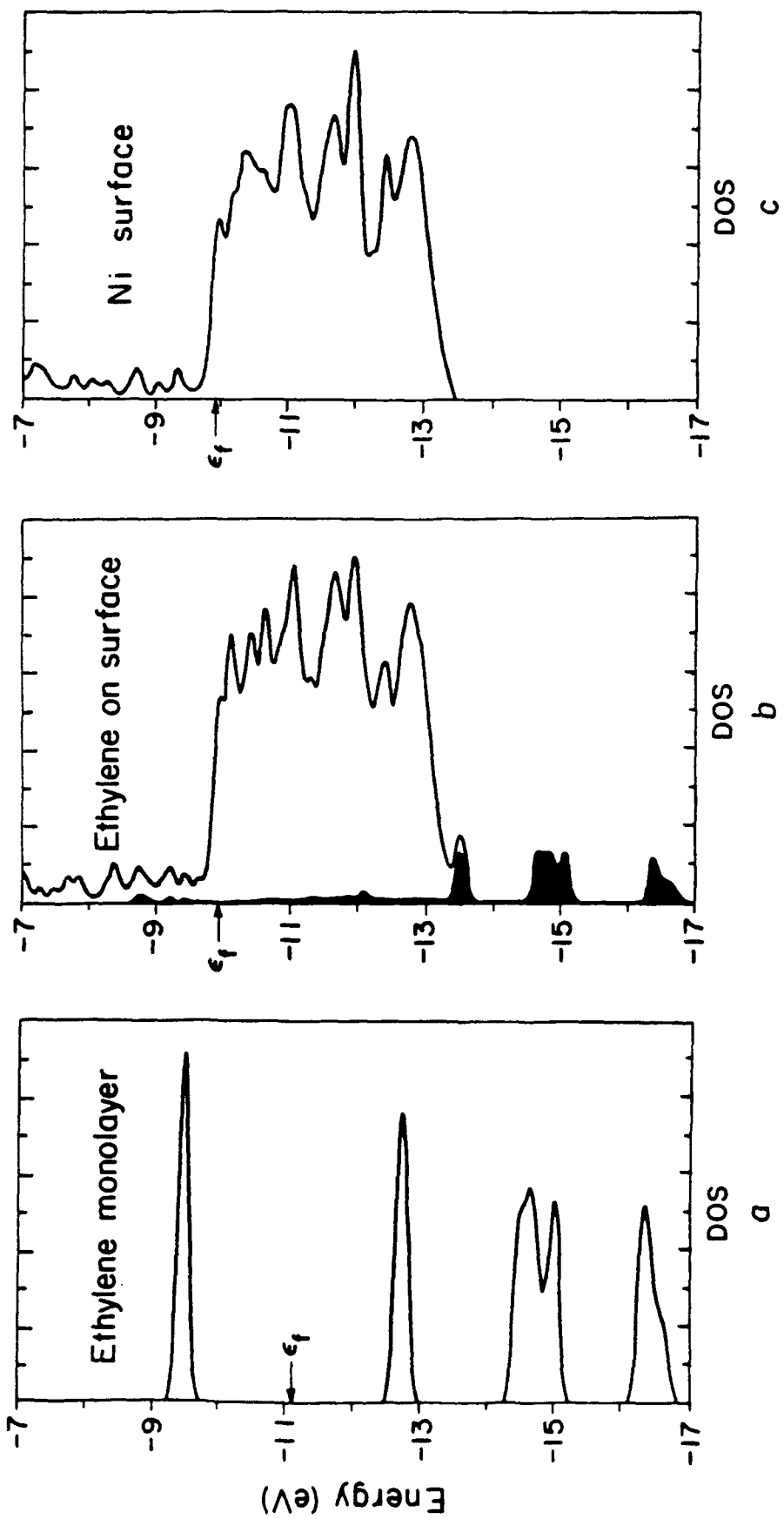


Figure 1. a) Total DOS of a monolayer of ethylene arranged in the same geometry as the adsorbed layer at Ni(2-fold).  
 b) Total DOS of ethylene (shaded) at Ni(2-fold) at one-quarter coverage.  
 c) Total DOS of Ni(111) surface.

---

Figure 2 here

---

Let us examine the bonding in these chemisorbed ethylenes by looking at the crystal orbital overlap population (COOP) curves in Figure 3. In the left panel are the COOP curves for the C-Ni bond. There are three important bonding regions defined in the left panel. Regions I and II consist of the bands near -14.5 eV and the sharp peak near -13.5 eV, respectively. Region III starts from the top of region II and goes up to the Fermi energy. Over 90% of the DOS of  $\sigma$  and  $\sigma_{\pi}$  can be found in the first region, while the  $\pi$  band is the major component of region II. A substantial amount of the DOS of  $\pi$  (~10%), and nearly all the DOS of  $\pi^*$  that is below the Fermi energy, is located in region III. The bonding in region II is almost entirely due to  $\pi$ -to-metal forward donation, while in region III it is mainly the result of metal-to- $\pi^*$  back-bonding and partly that of forward donation involving  $\pi$ .

---

Figure 3 here

---

A similar distribution of the DOS of the four frontier orbitals among the three bonding regions occurs at the on-top site of Ni(111) and the other two metal surfaces, Pd(111) and Pt(111). There are, however, two major trends. The DOS of  $\pi^*$  in region III decreases from the 2-fold site to the on-top site. For a given adsorption site, it increases in the following order: Pd(111)  $\rightarrow$  Pt(111)  $\rightarrow$  Ni(111).

We can partition the contributions to adsorbate-surface bonding by energy region; this and other bonding information is listed in Table 5. From the electron population of  $\pi$  and  $\pi^*$ , the strongest forward donation and back-bonding seem to occur at the 2-fold site of Ni(111) and Pt(111), respectively.

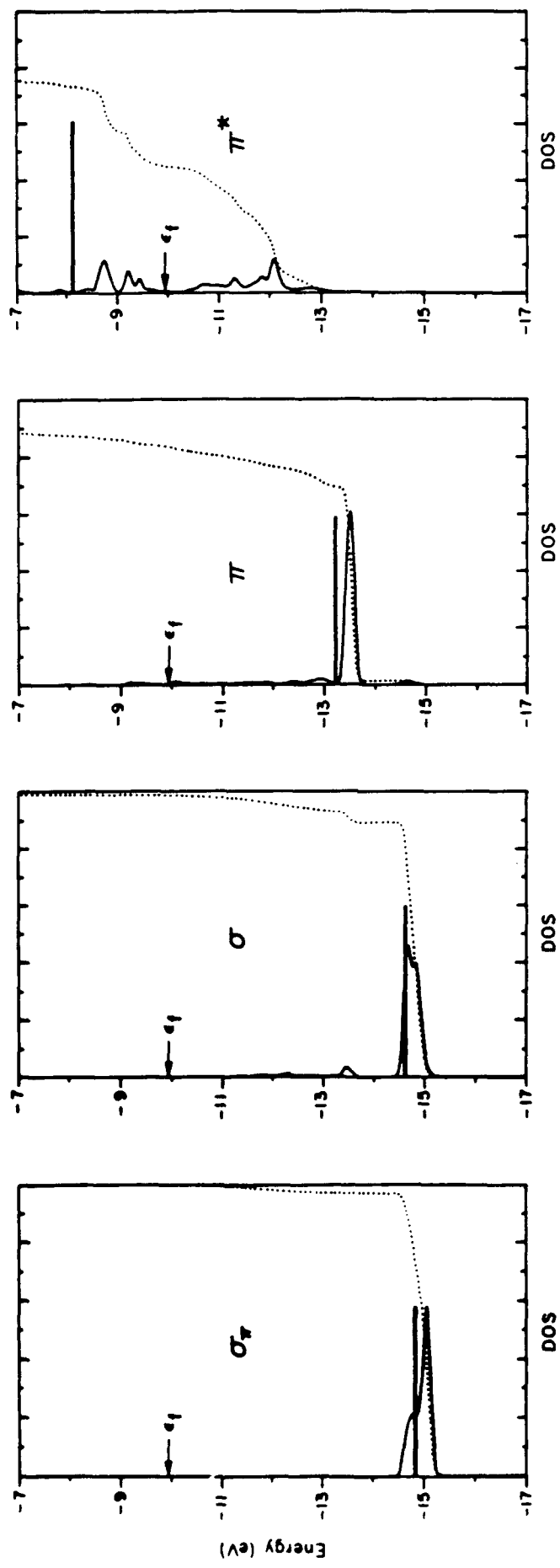


Figure 2. Projected DOS of the four frontier orbitals of ethylene at Ni(2-fold). The solid line and the dotted line are the DOS and integration curve respectively.

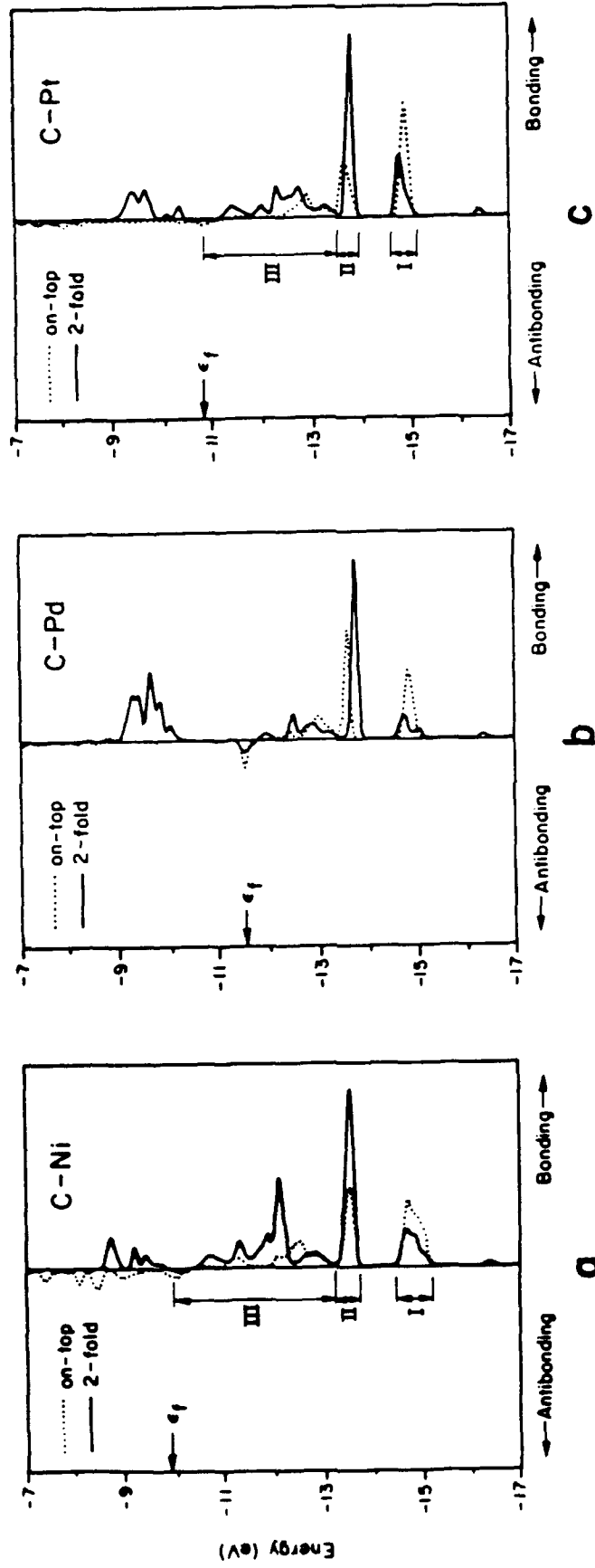


Figure 3. a) COOP curve for C-Ni bond.  
 b) COOP curve for C-Pd bond.  
 c) COOP curve for C-Pt bond.

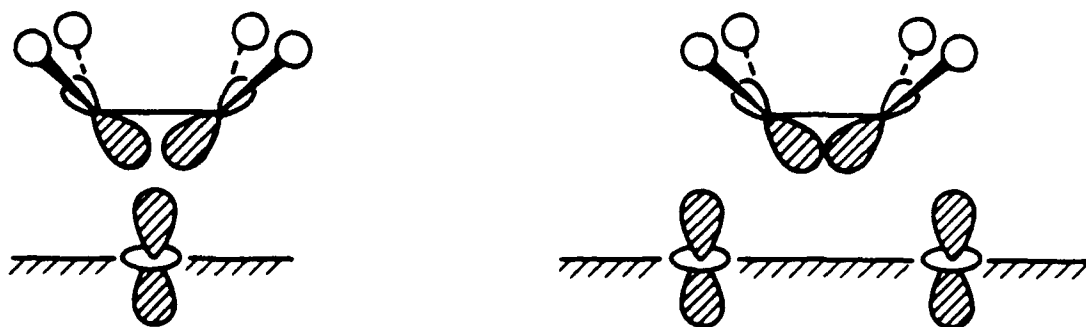
---

Table 5 here

---

The change in dispersion and electron occupation of  $\sigma$  and  $\sigma_{\pi}$  is not dramatic. Does this mean that  $\sigma$  and  $\sigma_{\pi}$  do not participate significantly in bonding to the surface? Although  $\sigma$  and  $\sigma_{\pi}$  show little change in electron occupation and do not develop substantial dispersion, they do interact with the surface, especially at the on-top site. For example, region I accounts for about 17% of the C-Pd OP at Pd(2-fold) but 44% at Pd(on-top). The COOP curves of Pt(on-top) in Figure 3 shows that the bonding peak in region I is actually larger than that in region II.

Our next goal is to determine whether  $\sigma$  or  $\sigma_{\pi}$  is the major source of ethylene-metal bonding in this region. From its shape,  $\sigma$  should overlap much better with the metal orbitals at the on-top site, as shown in 7. The reverse should be true for  $\sigma_{\pi}$ , because at



7

the on-top site it is locally orthogonal to all orbitals of the nearest metal atoms. From the OP in Table 5 and the COOP curves in Figure 3, the ethylene-metal interaction in region I decreases on going from the on-top to the 2-fold site, suggesting the dominance of  $\sigma$  over  $\sigma_{\pi}$ . This was confirmed by a numerical experiment, in which selected atomic overlaps

Table 5. Selected Bonding Information at the 2-fold site and the atop site.

	2-fold site			atop site		
	Ni(111)	Pd(111)	Pt(111)	Ni(111)	Pd(111)	Pt(111)
Net charge on chemisorbed ethylene	-0.55	+0.03	-0.19	-0.31	+0.06	-0.04
electron occupation of $\pi^*$	0.89	0.32	0.69	0.60	0.24	0.43
electron occupation of $\pi$	1.68	1.65	1.54	1.74	1.71	1.66
electron occupation of $\sigma$	1.98	1.99	1.97	1.950	1.96	1.93
electron occupation of $\sigma_\pi$	1.99	1.99	1.99	1.99	1.99	1.99
total carbon-metal overlap population (OP)	0.371	0.212	0.394	0.229	0.165	0.271
carbon-metal OP from region III	0.159	0.044	0.141	0.064	0.036	0.070
carbon-metal OP from region II	0.130	0.123	0.139	0.069	0.076	0.074
carbon-metal OP from region I	0.055	0.035	0.068	0.096	0.072	0.114
Fermi level in eV	-9.93	-11.53	-10.86	-9.91	-11.53	-10.86

between the surface and the adsorbate (those involved in  $\sigma_\pi$ ) were dropped.

Since  $\sigma$  is quite important at the on-top site of Pd(111) (in region I, it accounts for 42% of the total C-Pd OP), it is worthwhile to trace down the metal orbital that interacts strongly with it. Considering its orientation, a good candidate is  $d_{z^2}$  ( $s$  and  $p_z$  are eliminated because they would lead to substantial depopulation of  $\sigma$ ). As shown in Figure 4, region I picks up about 8% of the DOS of nearest surface  $d_{z^2}$  orbital at Pd(on-top). Even in the absence of the adsorbate, the  $s$ ,  $p_z$  and  $d_{z^2}$  of the surface atoms have the same symmetry and extensive hybridization is possible. It is therefore not a good idea to estimate the OP due to  $d_{z^2}$  by dropping the overlap. Instead we project out its contribution. In this way, mixing of orbitals induces no error. The projected OP for  $d_{z^2}$  is in region I is 0.043. The total projected OP for all other metal orbitals is 0.030. The interaction of  $\sigma$  with the  $d_{z^2}$  in this region is thus significantly greater than that of the total of the other eight metal orbitals.

---

Figure 4 here

---

$\pi$  and  $\pi^*$  are the most active participants in the adsorbate-surface interaction in region II and III. They undergo significant depopulation and population, respectively, upon adsorption. Their electron occupations also determine the net charge on the adsorbate, which is roughly equal to two minus their total electron population (see Table 5). On Ni(111) and Pt(111), the metal-to- $\pi^*$  back-donation of electron outweighs the forward donation from  $\pi$  and the adsorbed ethylene is negatively charged. The opposite occurs on Pd(111). As mentioned before, this may be due to its lower  $d$  bands. Notice that the  $\sigma$  band is always below the  $d$  block. A lower  $H_{ii}$  for the  $d$  orbitals means a better energy match for interaction. The percentage contribution of  $\sigma$  in region I to the metal-carbon OP is indeed greatest at the on-top site of Pd(111).

Detailed analysis of region II and III, however, is not so simple because it involves

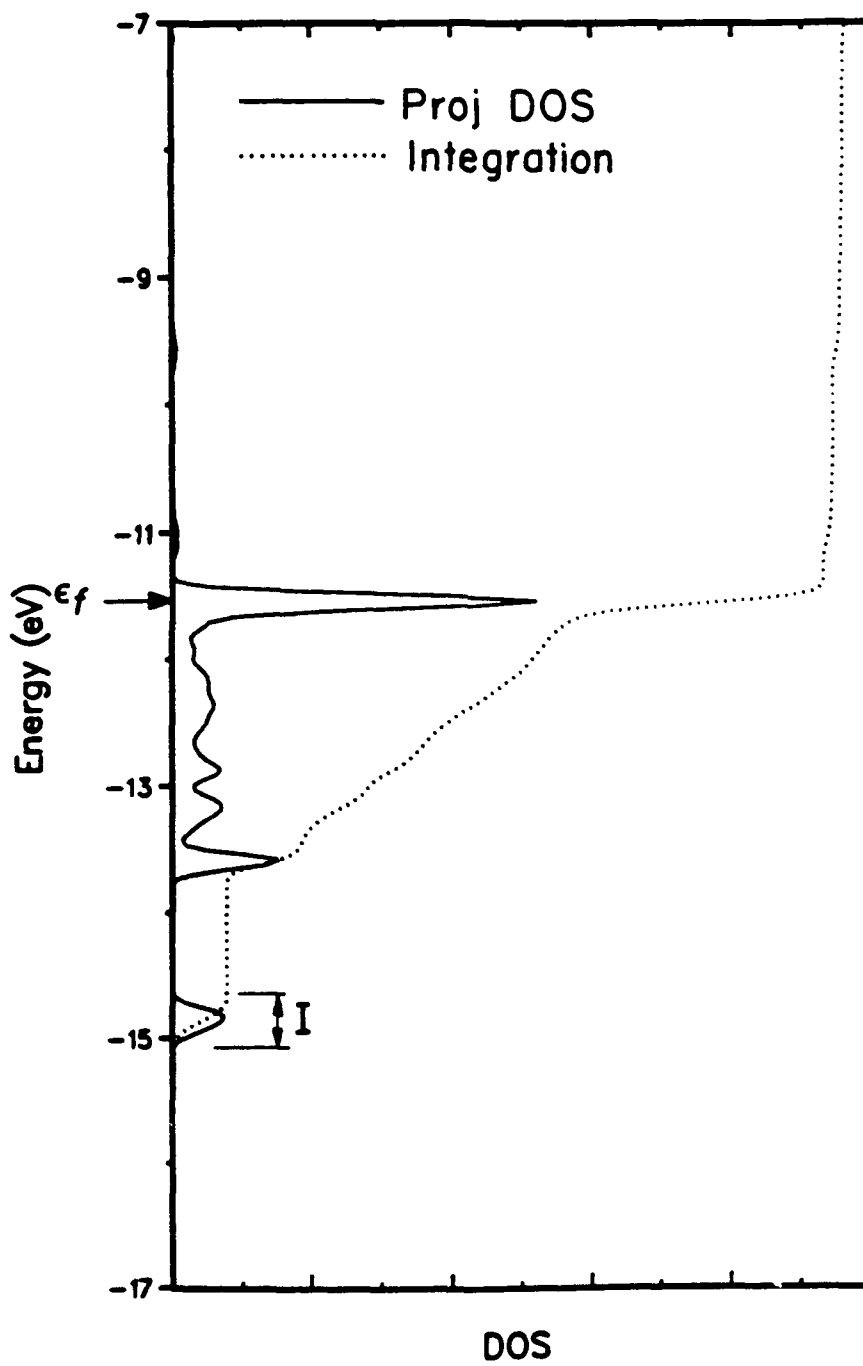


Figure 4. Projected DOS and integration curve for the  $d_{z^2}$  orbital of  $Pd_1$ .

contributions from  $\sigma$ ,  $\pi$  and  $\pi^*$ , some bonding, some antibonding. The analytical tools we have used so far may not give us a sufficiently detailed picture of adsorbate-surface interaction. What we need is a method to project out the individual contribution from each FMO of ethylene to the carbon-metal OP. In Table 6, the result of partitioning of the total carbon-metal overlap populations by this method is presented.

---

Table 6 here

---

Table 6 reveals several bonding features. First, we recall that there is strong interaction between  $\sigma$  and the metal surfaces at the on-top site. The  $\sigma$ -metal OP's, however, are not significant. In interpreting this apparent paradox, the  $\sigma$ -Pd COOP curve of Pd(on-top) in Figure 5 is instructive. The bonding peak in region I is essentially neutralized by antibonding interaction in region II and III. Although there are good overlaps between  $\sigma$  and the d orbitals, the net effect is almost nonbonding. The fact that there is a substantial amount of DOS of  $d_{z^2}$  in resonance with that of  $\sigma$  only means strong interaction but not necessarily strong bonding. To have strong bonding, the antibonding counterpart has to be above the Fermi energy. This is exactly what happens when  $\pi$  and  $\pi^*$  interact with the metal. An analysis of bonding that is solely based on the DOS thus may be insufficient.

---

Figure 5 here

---

On Ni(111), probably because of the higher Fermi energy,  $\pi^*$  always contributes more to the metal-carbon overlap population than  $\pi$ . The opposite occurs on Pd(111). For Pt(111), a transition can be observed: at the on-top site,  $\pi$  is more important, but at the 2-fold site  $\pi^*$  is the major source of C-Pt bonding. According to the electron populations in Table 5, the COOP curves in Figure 3 and the projected OP, the interaction of  $\pi$  and  $\pi^*$

Table 6. Contribution of the four FMO's of Ethylene to the Carbon-metal Overlap Populations. The contributions of the other eight FMO's are negligible.

FMO	2-fold site			atop site		
	Ni(111)	Pd(111)	Pt(111)	Ni(111)	Pd(111)	Pt(111)
$\pi^*$	0.236	0.108	0.215	0.118	0.072	0.113
$\pi$	0.137	0.119	0.172	0.108	0.118	0.140
$\sigma$	-0.001	-0.003	0.001	0.032	0.018	0.043
$\sigma_\pi$	-0.005	-0.002	-0.003	-0.002	-0.001	-0.002
Total metal-carbon overlap population	0.371	0.212	0.394	0.229	0.165	0.271

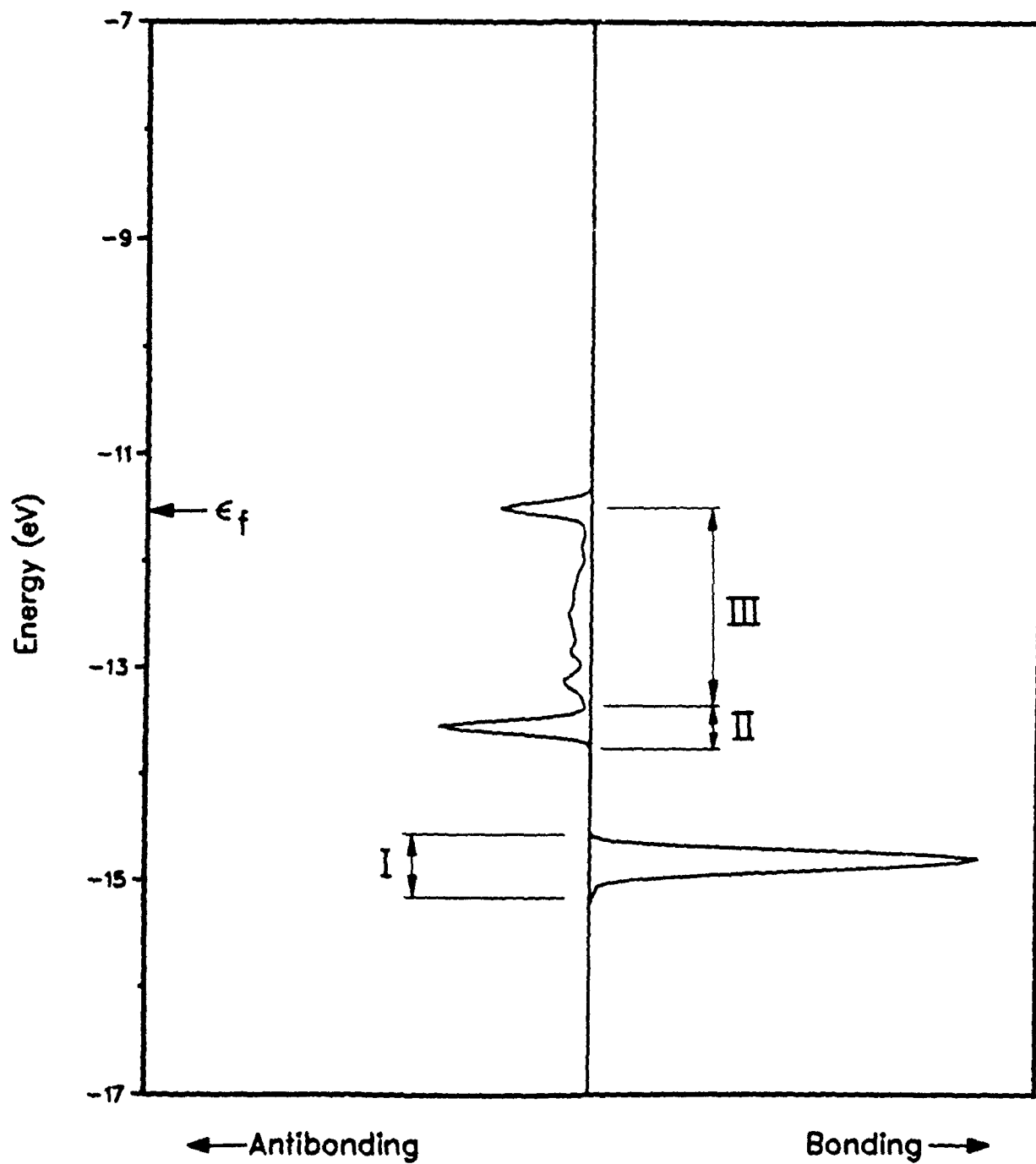


Figure 5.  $\sigma$ -Pd<sub>1</sub> COOP curve.

with the metal surface strengthens on going from the on-top site to the 2-fold site. This may be a combination of two factors: orientation and symmetry. The lobes of  $\pi$  and  $\pi^*$  are pointing towards the metal atoms at the 2-fold site but away from them at the on-top site, 8.



8

For a  $\pi$ -bonded ethylene, symmetry prevents any good overlap between  $\pi$  and the nearest metal  $p_x$  and  $d_{xz}$ . It also prohibits any effective interaction of  $\pi^*$  with the surface  $s$ ,  $p_z$  and  $d_{z^2}$ , 9. There is another interesting but more subtle feature concerning  $\pi^*$ . For



9

Ni(111) and Pt(111), the  $\pi^*$ -Ni<sub>1</sub> and  $\pi^*$ -Pt<sub>1</sub> OP decrease significantly ( 50% for the former and 46% for the latter), on changing from a di- $\sigma$ -bonded ethylene to a  $\pi$ -bonded adsorbate. The corresponding reduction of OP on Pd(111) is much smaller, only about 8%. In addition, if we compare the electron occupation of  $\pi^*$  between the two adsorption sites among the three metal surfaces, again there is a much smaller difference on Pd(111).

This differential weakening of  $\pi^*$ -metal interaction may be understood by examining Figure 6. In the left panel are the COOP curves for  $\pi^*$ -Pd<sub>1</sub> at Pd(2-fold) and Pd(on-top). By projecting out the OP between  $\pi^*$  and individual palladium orbitals, it is found that the two bonding peaks at -12.5 eV (within region III) are mainly the result of interaction between  $\pi^*$  and  $d_{xz}$  at the on-top site;  $\pi^*$ ,  $d_{z^2}$  and  $d_{xz}$  at the 2-fold site. These two peaks are of similar size and hence the similar  $\pi^*$ -Pd<sub>1</sub> OP at Pd(2-fold) and Pd(on-top). Near -9.5 eV, where most of the DOS of  $\pi^*$  is located, the situation is completely different. For Pd(on-top), there is some  $\pi^*$ - $p_x$  bonding interaction which is almost exactly cancelled out by the antibonding interaction between  $\pi^*$  and  $d_{xz}$ . The net result is that the orbitals in this region are mainly  $\pi^*$ -Pd nonbonding. For Pt(2-fold), the bands near -9.5 eV are  $\pi^*$ - $d_{xz}$  and  $\pi^*$ - $d_{z^2}$  antibonding but  $\pi^*$ - $s$ ,  $\pi^*$ - $p_z$  and  $\pi^*$ - $p_x$  bonding. The bonding interactions of  $s$  and  $p$  outweigh the antibonding interactions of the  $d$  and a prominent bonding peak appears. ( This peak actually is larger than that in region III).

---

Figure 6 here

---

In summary, the  $\pi^*$ -Pd bonding at the on-top site may be represented schematically by a 'three-level' interaction diagram in 10. A characteristic outcome of this type of interaction is a nonbonding level in the middle. In this case, it corresponds to the  $\pi^*$

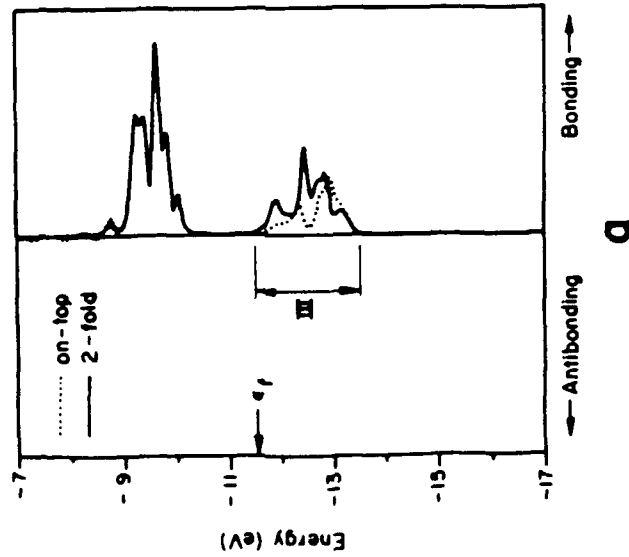
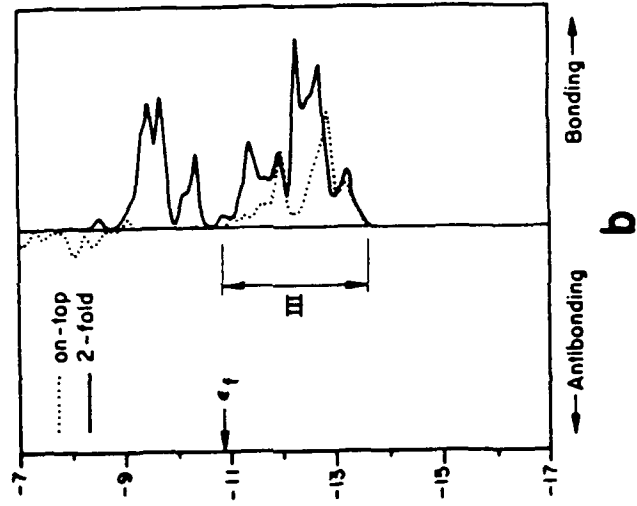
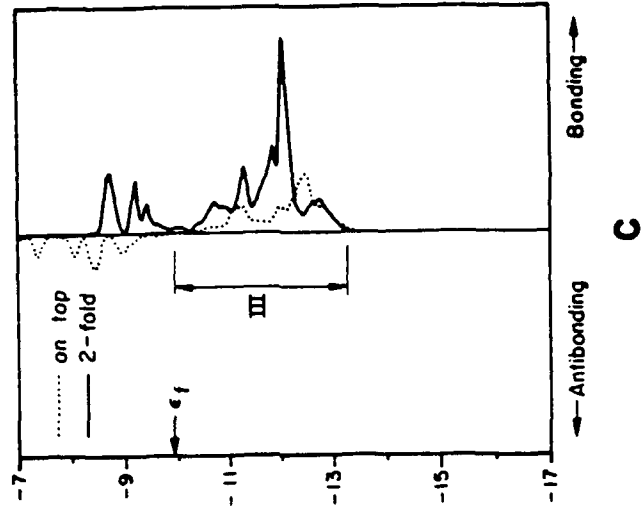
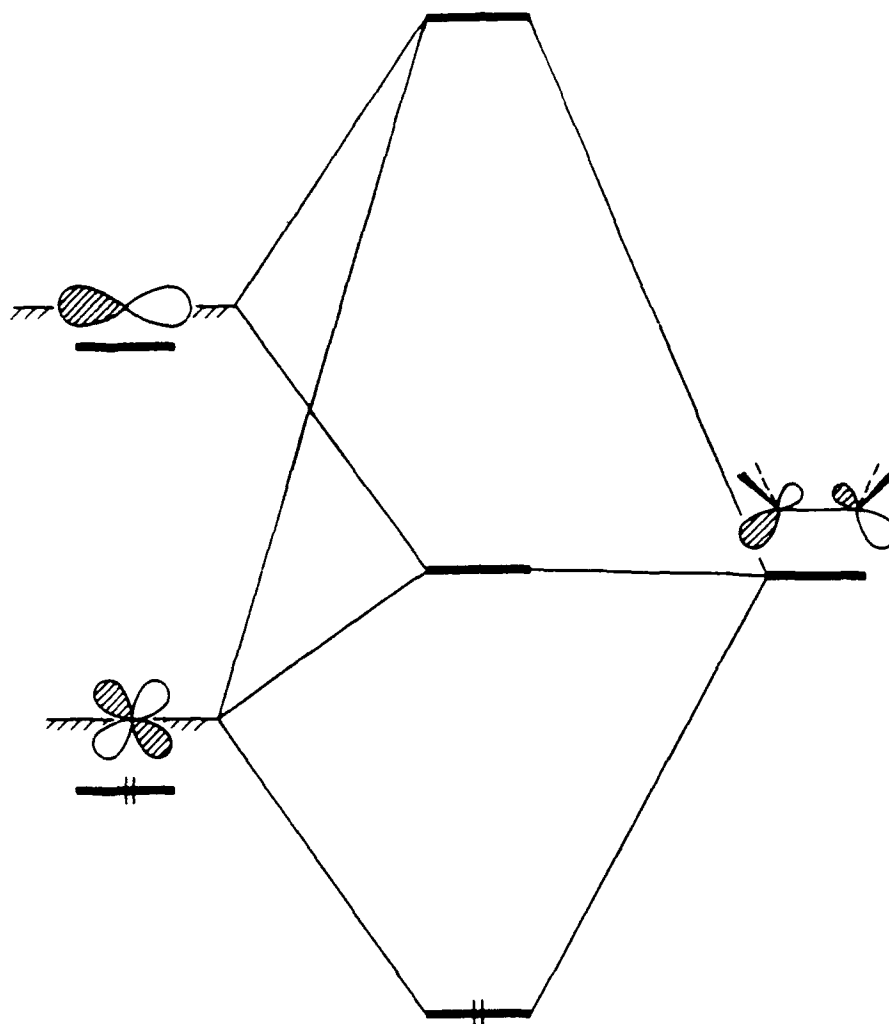
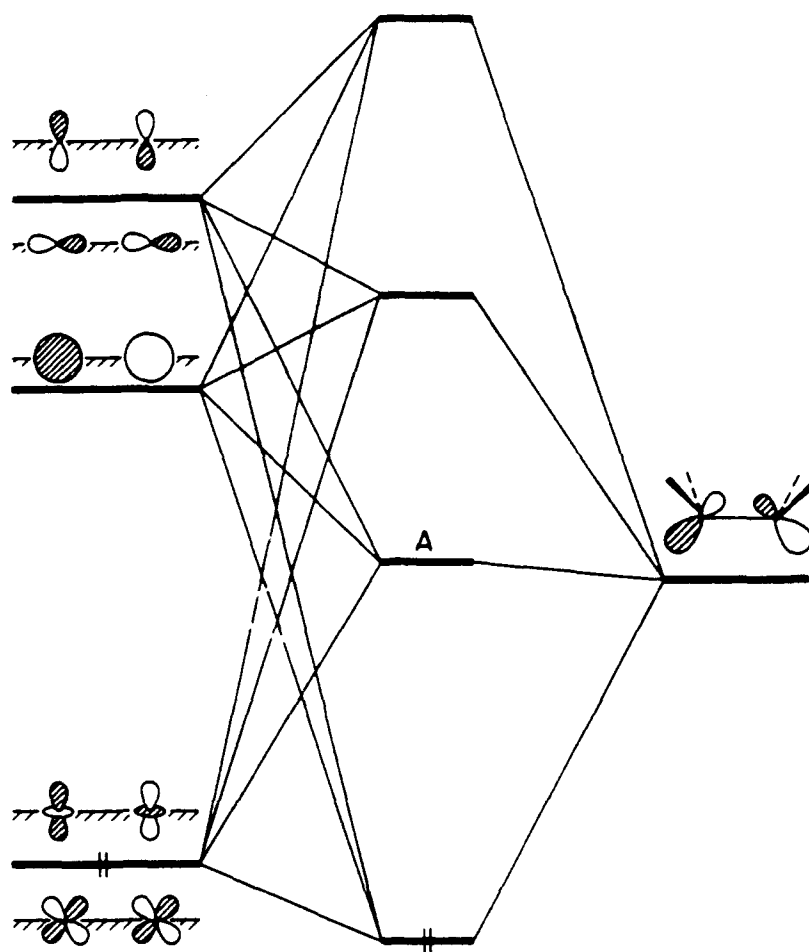


Figure 6. a)  $\pi^*$ -Pd COOP curve.  
 b)  $\pi^*$ -Pt COOP curve.  
 c)  $\pi^*$ -Ni COOP curve.



10

orbitals just above the Fermi energy. At the 2-fold site, if we consider  $p_x$  and  $p_y$  as one level,  $d_{xz}$  and  $d_{z^2}$  as another, a 'four-level' interaction diagram of the type shown in 11 may be appropriate to describe the  $\pi^*$ -Pd bonding. The second level, which is labelled as A, is the cause of the large bonding peak near -9.5 eV. The orbitals on the left side of this drawing are meant to remind the reader that  $\pi^*$  can overlap effectively only with those metal orbitals that are  $Pd_1$ - $Pd_2$  antibonding.



11

The  $\pi^*$ -Pt<sub>1</sub> COOP curves are displayed in the middle panel of Figure 6. Part of A has been pushed down below the Fermi energy and the bonding peak near -9.5 eV is smaller than that in region III. The result is dramatic. In Pd(2-fold), the s and p bands only account for 27% of the  $\pi^*$ -Pd OP but in Pt(2-fold), their contribution to the  $\pi^*$ -Pt OP is about 50%. The  $\pi^*$ -surface bonding in the upper part of region III is dominated by the s and p bands. For Ni (111), as indicated by the COOP curves in the right panel, an even larger portion of A has penetrated into region III. Now over 59% of the  $\pi^*$ -Ni OP can be

attributed to the s and the p orbitals. These results also fit the general trend that the chemistry of palladium is more similar to that of platinum than nickel.<sup>26</sup>

Thus, it is the position of A relative to the Fermi energy that is mainly responsible for the differential reduction in the OP between  $\pi^*$  and the nearest surface atom on going from the 2-fold to the on-top site. The incapability of the s and p orbitals of the palladium to push A down below the Fermi energy greatly diminishes the back-bonding, and Pd(2-fold) is the only 2-fold site at which  $\pi$  contributes more to the carbon-metal OP than  $\pi^*$ .

A more thorough, quantitative description of the bonding of  $\pi$  and  $\pi^*$  with the metal orbitals is given in Table 7 and 8. Due to a symmetry constraint, almost half of the OP in these two tables are equal or close to zero. The OP's in Table 7 clearly show that the  $\pi$ -surface bonding occurs mainly via the metal s and p bands, in agreement with the concept of forward donation. Similarly, the idea of back-bonding is well illustrated by the results in Table 8.

---

Table 7 and 8 here

---

So far, we have concentrated on the adsorbate. How about the surfaces? Generally, the greater the number of surface atoms directly bonded to the adsorbate, the greater will be the bond-weakening within the surface. The metal-metal OP's, however, indicate that the degree of bond weakening at the surface for the on-top and 2-fold site is essentially the same, that is, this factor is not crucial in determining the site preference. As we shall see in a future paper, such is not the case if the adsorbate is carbon monoxide. One would like to separate the carbon-metal OP into nine components, corresponding to the contribution of each orbital of the metal atoms involved in anchoring the ethylene. The s and p bands of a transition metal are very diffuse. Their band-widths are tens of eV. The changes in DOS of these orbitals after adsorption are thus much less obvious than those of

Table 7. Overlap Population between  $\pi$  and the Nine Metal Surface Orbitals. The  $p_y$ ,  $d_{xy}$ ,  $d_{yz}$  interactions vanish by local symmetry, and are not listed.

metal orbital	2-fold site			atop site		
	Ni(111)	Pd(111)	Pt(111)	Ni(111)	Pd(111)	Pt(111)
s	0.075	0.082	0.082	0.067	0.085	0.077
$p_x$	0.001	0.002	0.003	0	0	0
$p_z$	0.042	0.031	0.050	0.0290	0.027	0.039
$d_{x^2-y^2}$	0	0	0	-0.001	-0.001	-0.001
$d_z^2$	0.016	0.004	0.028	0.013	0.006	0.025
$d_{xz}$	0.003	0.001	0.009	0	0	0

Table 8. Overlap Population between  $\pi^*$  and the Nine Metal Surface Orbitals. The  $p_y$ ,  $d_{xy}$ ,  $d_{yz}$  interactions vanish by local symmetry, and are not listed.

metal orbital	2-fold site			atop site		
	Ni(111)	Pd(111)	Pt(111)	Ni(111)	Pd(111)	Pt(111)
s	0.078	0.017	0.061	0	0	0
$p_x$	0.003	0.003	0.004	0.018	0.005	0.017
$p_z$	0.058	0.009	0.043	0	0	0
$d_{x^2-y^2}$	-0.001	-0.001	-0.001	0	0	0
$d_{z^2}$	0.087	0.059	0.084	-0.001	0	0
$d_{xz}$	0.010	0.020	0.023	0.100	0.067	0.097

the d bands. As a result, the role of the s and p orbitals on chemisorption involving transition metals is seldom discussed, although, by analogy to organometallic compounds, these orbitals should interact with the adsorbate. Their counterparts, the more contracted d orbitals, may be over-emphasized in the existing literature discussions, including our own. The partitioning of the carbon-metal OP (Table 9) may provide more insight on this issue.

---

Table 9 here

---

There is little doubt that the d orbitals are involved in adsorbate-surface bonding, but the combined effect of the s and p bands is much more important. In fact, apart from the on-top site on Ni(111), the s orbital alone contributes more to the carbon-metal OP than the total of the five d orbitals. As shown by the OP in Table 7 and 8, the reason behind this is that, apart from forward donation, the surface s and p bands participate actively in  $\pi^*$ -metal bonding. In all adsorption sites,  $p_y$ ,  $d_{xy}$  and  $d_{yz}$  are orthogonal to  $\sigma$ ,  $\pi$  and  $\pi^*$ . Most of the interaction between  $p_x$  and metal surfaces occurs above the Fermi energy.  $d_{x^2-y^2}$  may engage heavily in metal-metal bonding. Hence these five orbitals only play a minor role in surface-adsorbate bonding.

The interaction between the ethylene and the surface s,  $p_z$  and  $d_{z^2}$  bands reduces substantially as one moves from the 2-fold to the on-top site. From the previous discussion, we think that this may be related to the symmetry of  $\pi^*$ . To confirm our conjecture, we take a close look at the COOP curves between Ni s and carbon in Figure 7. For the 2-fold site, there is significant bonding contribution from region III, indicative of strong interaction with the  $\pi^*$ .  $\pi^*$  is orthogonal to the nearest surface s orbital at the on-top site. Effective overlap is thus prohibited and the bonding interaction is much smaller. A similar argument seems to apply to the  $p_z$  and  $d_{z^2}$ .

Table 9. Contribution of the Nine Metal Orbitals to the Carbon-metal Overlap Populations.

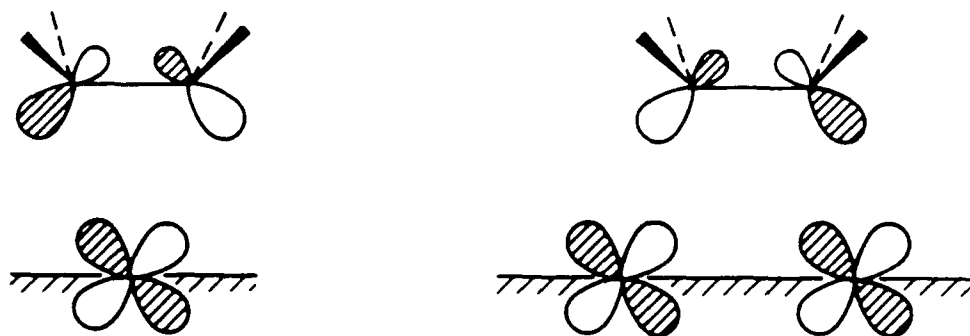
metal orbital	2-fold site			atop site		
	Ni(111)	Pd(111)	Pt(111)	Ni(111)	Pd(111)	Pt(111)
s	0.169	0.117	0.160	0.095	0.105	0.105
p <sub>x</sub>	0.004	0.005	0.010	0.019	0.007	0.019
p <sub>y</sub>	-0.001	-0.000	0.001	-0.002	-0.003	-0.001
p <sub>z</sub>	0.092	0.015	0.089	0.022	-0.000	0.036
d <sub>x<sup>2</sup>-y<sup>2</sup></sub>	-0.002	-0.002	-0.002	-0.001	-0.001	-0.001
d <sub>z<sup>2</sup></sub>	0.104	0.062	0.110	-0.003	-0.001	0.018
d <sub>xy</sub>	0.001	-0.000	0.000	-0.001	-0.0010	-0.001
d <sub>xz</sub>	0.010	0.020	0.031	0.101	0.067	0.097
d <sub>yz</sub>	-0.005	-0.005	-0.005	-0.000	-0.001	-0.001

---

Figure 7 here

---

In contrast to other metal orbitals, the projected OP of  $d_{xz}$  is much larger at the on-top site. To trace down the reason for this, we examine the COOP curves for the carbon atom and the Ni  $d_{xz}$  in the left panel of Figure 8. At the on-top site,  $d_{xz}$  is orthogonal to  $\sigma$ ,  $\sigma_\pi$  and  $\pi$  of ethylene. The interactions in the first two regions are thus negligible. For the 2-fold site, the symmetry constraint is partially relaxed.  $\sigma$ ,  $\pi$  and the part of the surface  $d_{xz}$  band that is  $Ni_1-Ni_2$  bonding undergo a 'three-level' interaction. However, the greatest difference occurs in region III. In Ni(2-fold),  $\pi^*$  can only overlap effectively with the upper part of the surface  $d_{xz}$  band that is  $Ni_1-Ni_2$  antibonding. In Ni(on-top), it can interact extensively with the whole  $d_{xz}$  band, as shown in 12. Thus a much larger C- $d_{xz}$



12

OP results (see Table 8). The COOP curve in the right panel is meant to illustrate the characteristics of the above 'three-level' interaction; the lowest level is strongly bonding, the middle level essentially nonbonding, and the third level strongly antibonding.

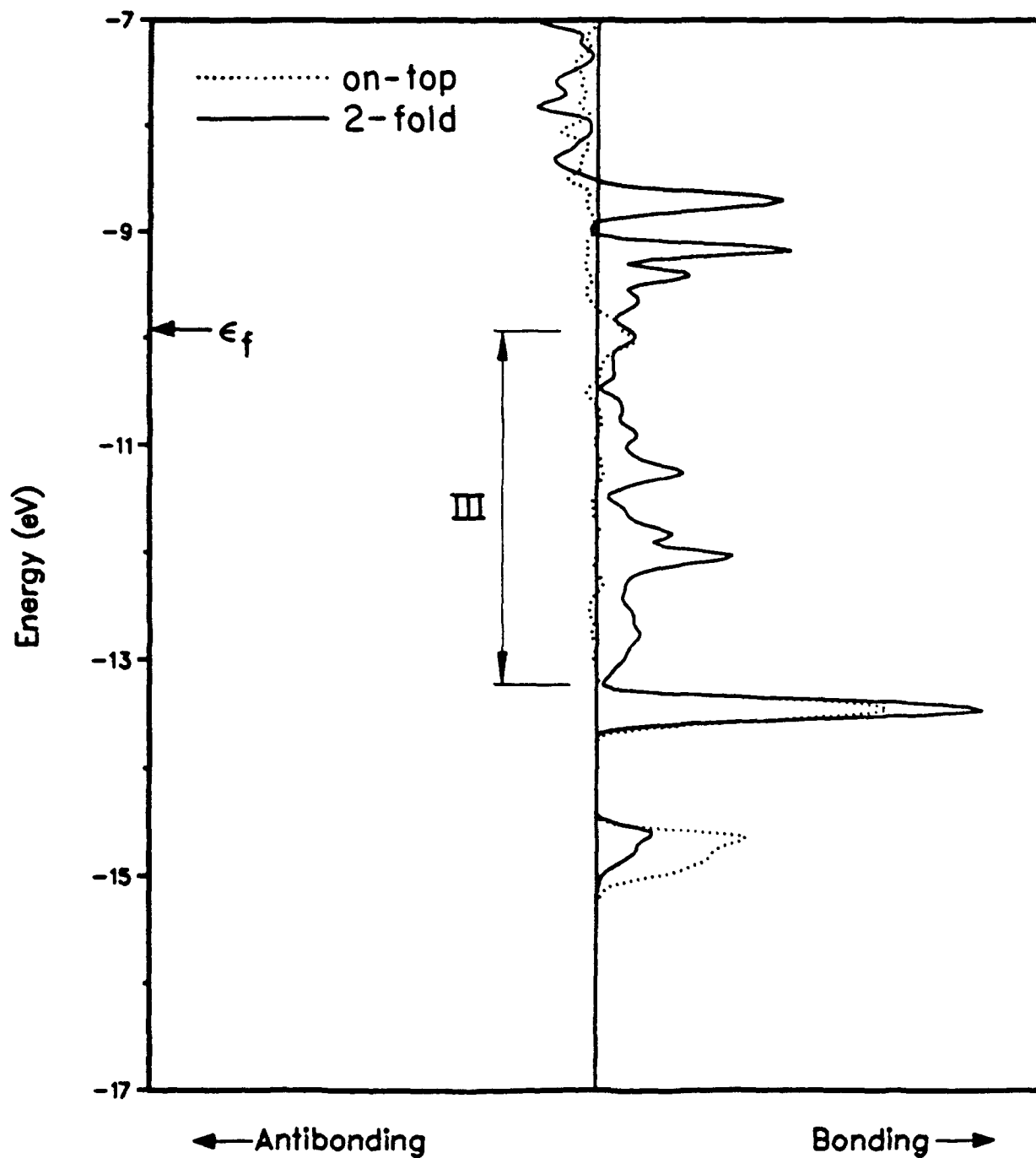


Figure 7. Contribution of the nickel s orbital to the Ni-C COOP curve.

---

Figure 8 here

---

It is instructive to examine the partitioning of the Ni-C COOP curves into the s, p and d components. As expected, in Figure 9 the s and p bands produce large bonding peaks in region II, where most DOS of  $\pi$  can be found, corresponding the  $\pi$ -to-metal forward donation. Surprisingly, this is also true for the d orbitals. This would induce some antibonding interaction within region III. Hence the unexpectedly small contribution of the d bands to the carbon-metal OP (relative to s and p) is due to the antibonding peaks in region III, as a direct result of interactions of the d bands with filled orbitals of ethylene. (We see here a surface analogue of the molecular two-level-four electron repulsion).<sup>3</sup> The partitioning of the C-Pd and C-Pt COOP curves shows similar features.

---

Figure 9 here

---

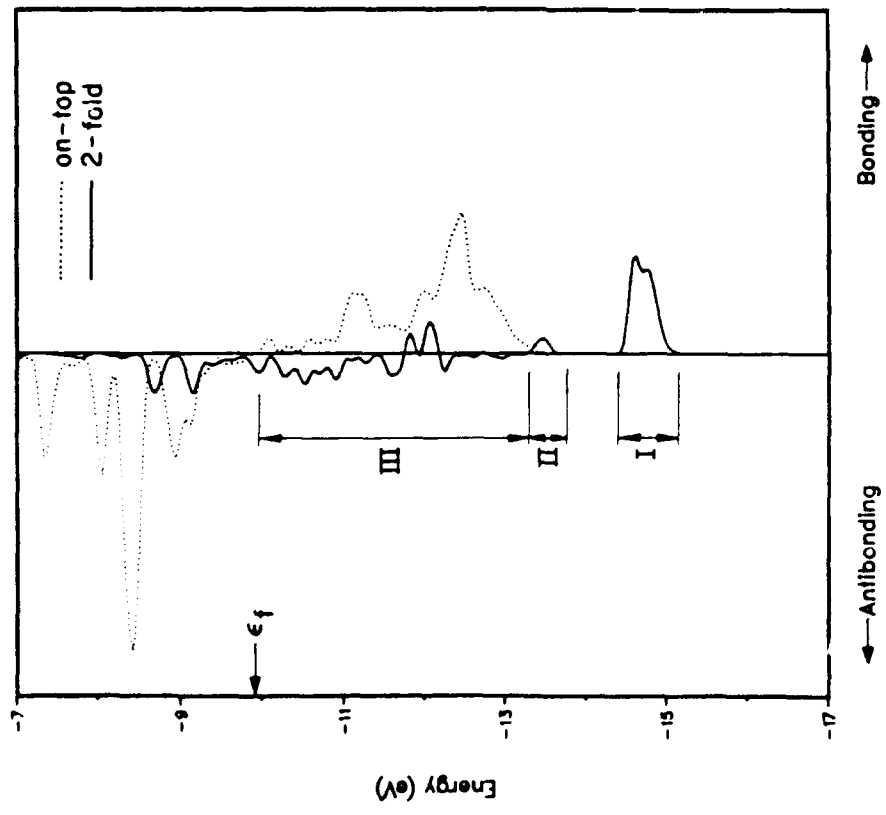
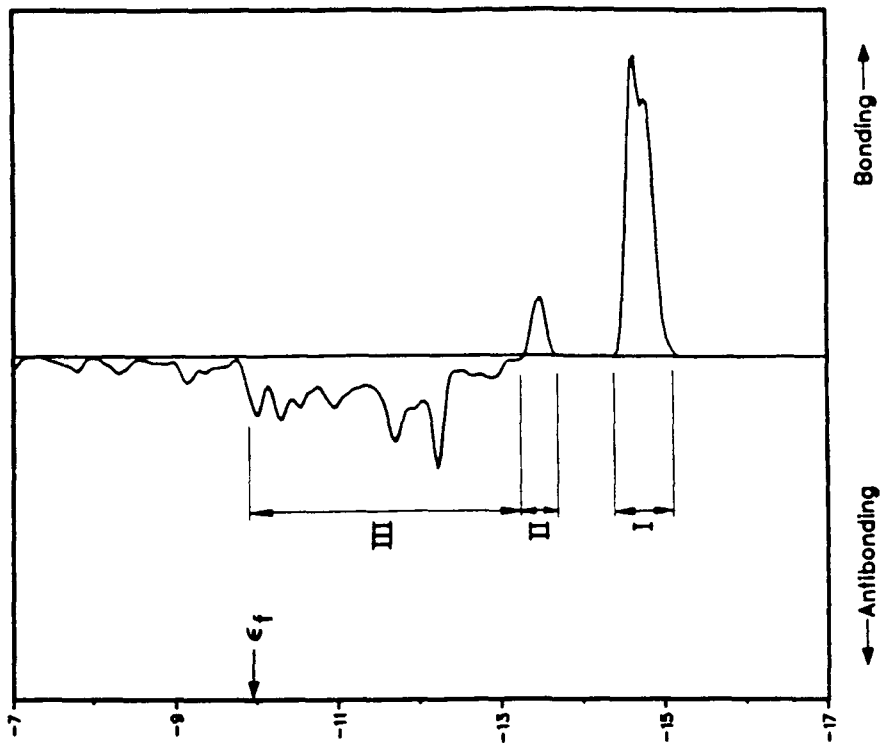


Figure 8. a) COOP curve for the  $d_{xz}$  orbital of surface nickel atoms and ethylene.  
 b) COOP curve for the interaction between the  $\sigma$  and  $\pi$  orbital of ethylene with the  $d_{xz}$  orbitals of the surface nickel atoms.

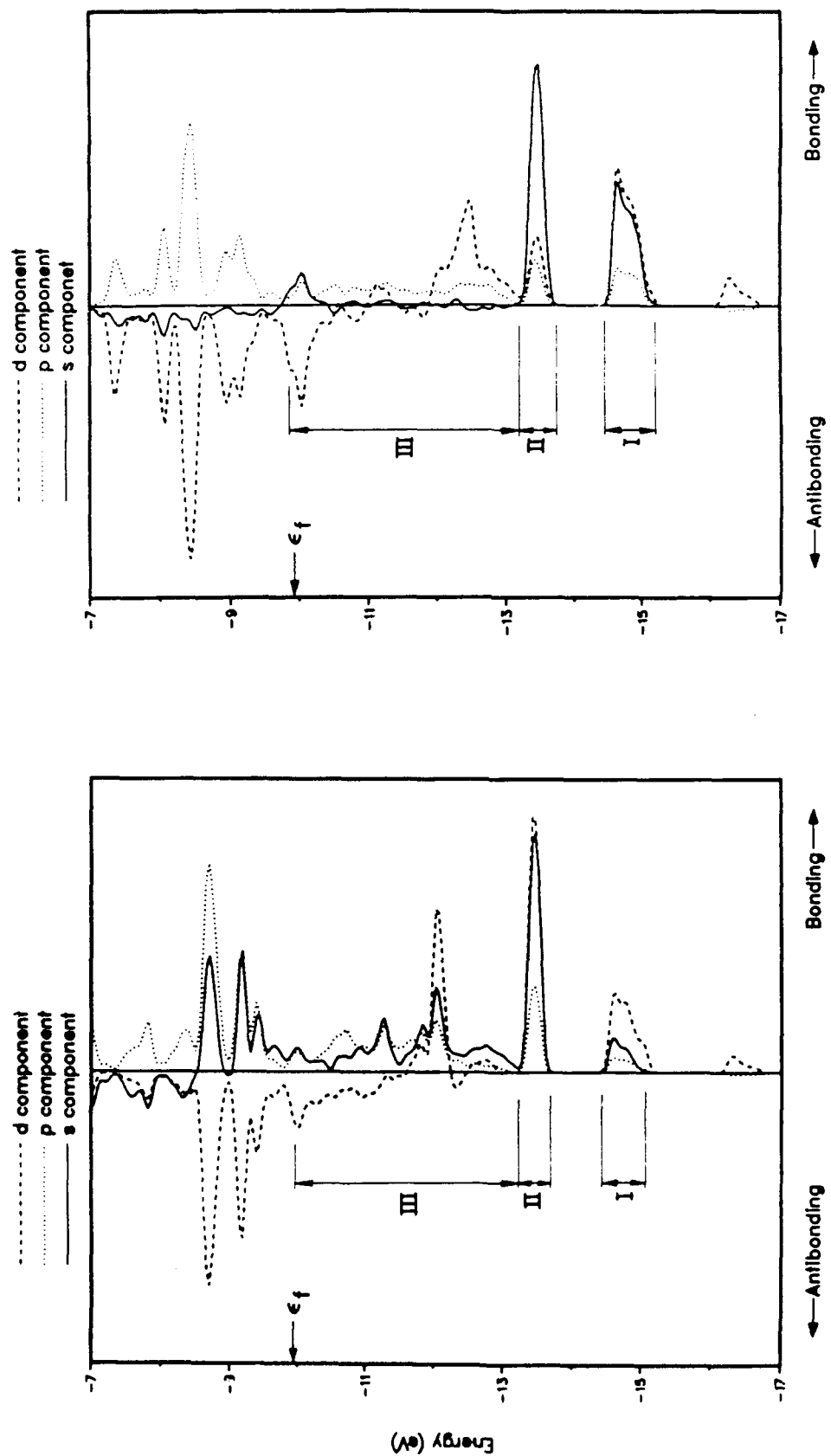
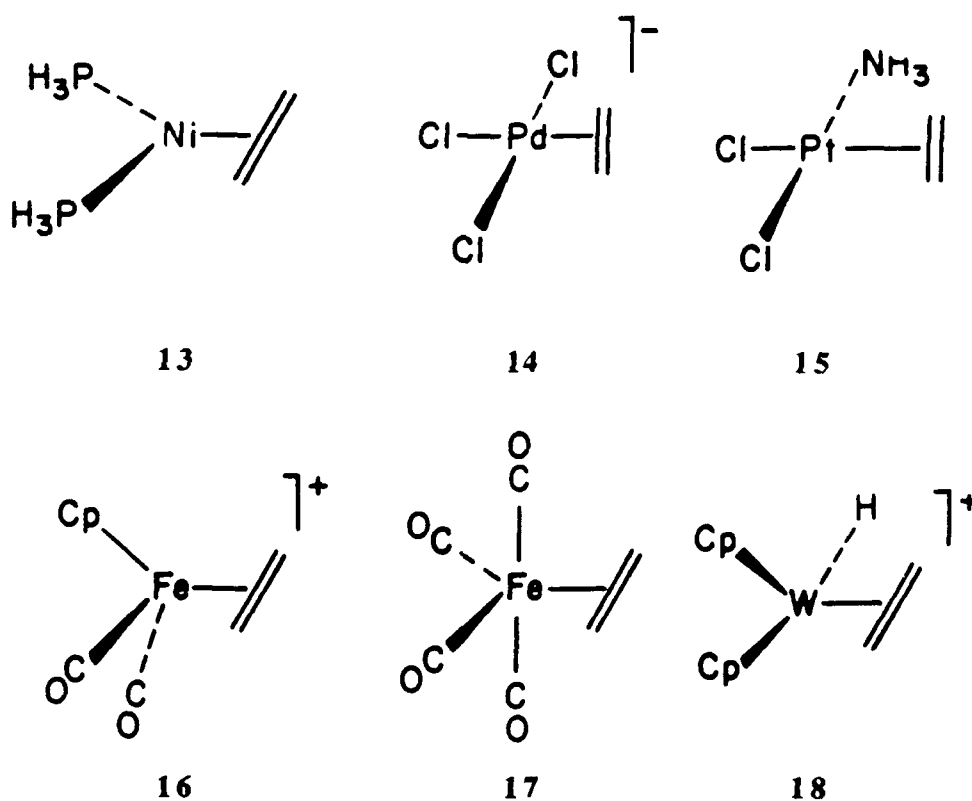


Figure 9. Partition of the C-Ni COOP curve for Ni(2-fold)(left) and Ni(on-top)(right).

## The Organometallic Analogy

It is instructive to compare the computational results for the three on-top sites with those of discrete, molecular  $\eta^2$  coordinated ( $\pi$ -bonded) olefinic complexes, studied in a previous paper of our group.<sup>33</sup> Unfortunately the ethylenes were kept planar in the molecular calculations, for reasons of simplicity. For comparison, we planarize our adsorbates and redo the calculations. Selected information is collected in Table 10, where the occupation of  $\pi$  and  $\pi^*$  of ethylene for molecules 13 - 18 is reported. Note that the



generally similar occupations for discrete molecules and surfaces for a given metal, and the wider range of occupations in known organometallic olefin complexes.

---

Table 10 here

---

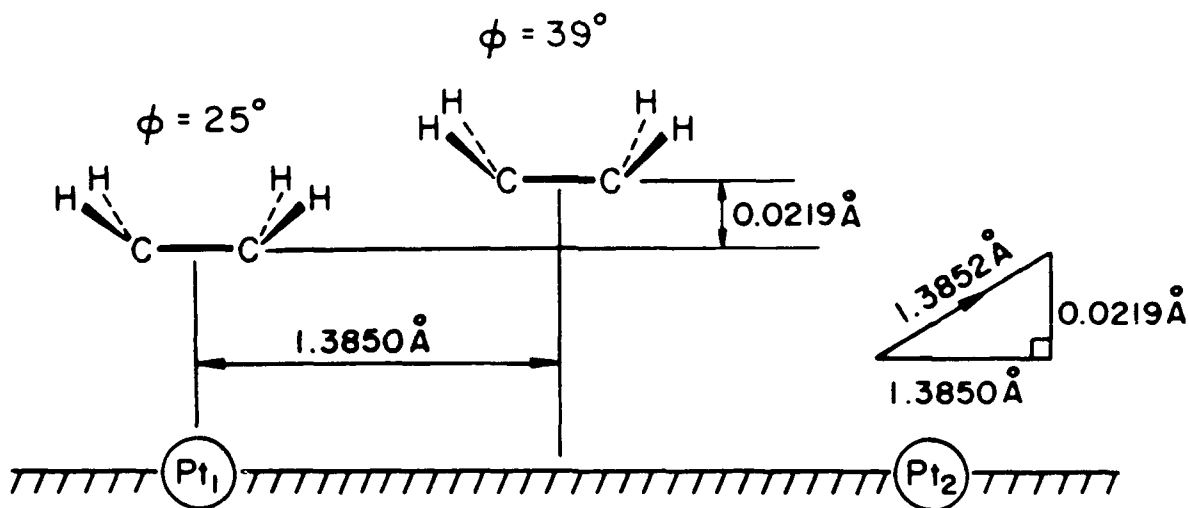
Table 10. Electron Density of  $\pi$  and  $\pi^*$  and the Net Charge on Ethylene.

System	$\pi$	$\pi^*$	Net Charge
Ni(PH <sub>3</sub> ) <sub>2</sub> C <sub>2</sub> H <sub>4</sub>	1.81	0.44	-0.28
Ni(on-top)	1.76	0.47	-0.27
(PdCl <sub>3</sub> C <sub>2</sub> H <sub>4</sub> ) <sup>-</sup>	1.71	0.21	+0.02
Pd(on-top)	1.66	0.35	+0.01
cis-PtCl <sub>2</sub> NH <sub>3</sub> C <sub>2</sub> H <sub>4</sub>	1.64	0.24	+0.10
Pt(on-top)	1.66	0.35	+0.01
CpFe(CO) <sub>2</sub> C <sub>2</sub> H <sub>4</sub> <sup>+</sup>	1.53	0.32	+0.20
Fe(CO) <sub>4</sub> C <sub>2</sub> H <sub>4</sub>	1.66	0.48	-0.15
Cp <sub>2</sub> WHC <sub>2</sub> H <sub>4</sub> <sup>+</sup>	1.74	0.60	-0.36

There are certainly many similarities between the organometallic compounds and surface complexes. Yet there are differences too. For instance, the energy of the HOMO depends strongly on the nature of the ligand, while the metal Fermi energy is not affected by the adsorbate molecules. The work function of the metal does vary after chemisorption, due to a change in the surface dipole. The similarities build the connections. The differences make each of them an exciting research subject on its own.

## Interconversion of $\pi$ -bonded to di- $\sigma$ -bonded ethylene

To our knowledge, there have been two reports on the transformation of a  $\pi$ -bonded ethylene to a di- $\sigma$ -bonded adsorbate on Pt(111).<sup>17,34</sup> We would like to estimate the activation energy of this process. Given our geometries, the transformation involves a translational motion of 1.3852 Å and an increase in the bending angle of the HCH plane ( $\phi$ , see 3) by 14°. We thus assume a reaction pathway in which there is an increase in 1.4° of bending angle for every linear translation of 0.13852 Å, 19. In Figure 10, we present the potential energy curve for this transformation. The activation energy was found to be 0.22 eV. Hence the transformation seem to be energetically feasible, this is a small energy.



19

By assuming a similar reaction pathway (one degree decrease in bending angle  $\phi$  per linear translation of 1.3752 Å), the activation energy for the conversion of the 2-fold site on Pd(111) to the on-top site was estimated to be 0.14 eV.

24

There have been some indications of the existence of a  $\pi$ -bonded ethylene on Pt(111),<sup>12,17,34</sup> Since the energy differences for the two adsorption sites on the two surfaces, Pd(111) and Pt(111) are similar (but in opposite order) and the activation energies for transformation are roughly the same, it may be worthwhile to try to detect the di- $\sigma$ -bonded species on Pd(111). On the contrary, the energy barrier for the transformation of ethylene from the on-top site on Ni(111) to the 2-fold site was calculated to be a tiny 0.0026 eV. The  $\pi$ -bonded species on Ni(111) seems to be thermodynamically and kinetically unstable with respect to the di- $\sigma$ -bonded ethylene and its detection, may be more difficult.

---

Figure 10 here

---

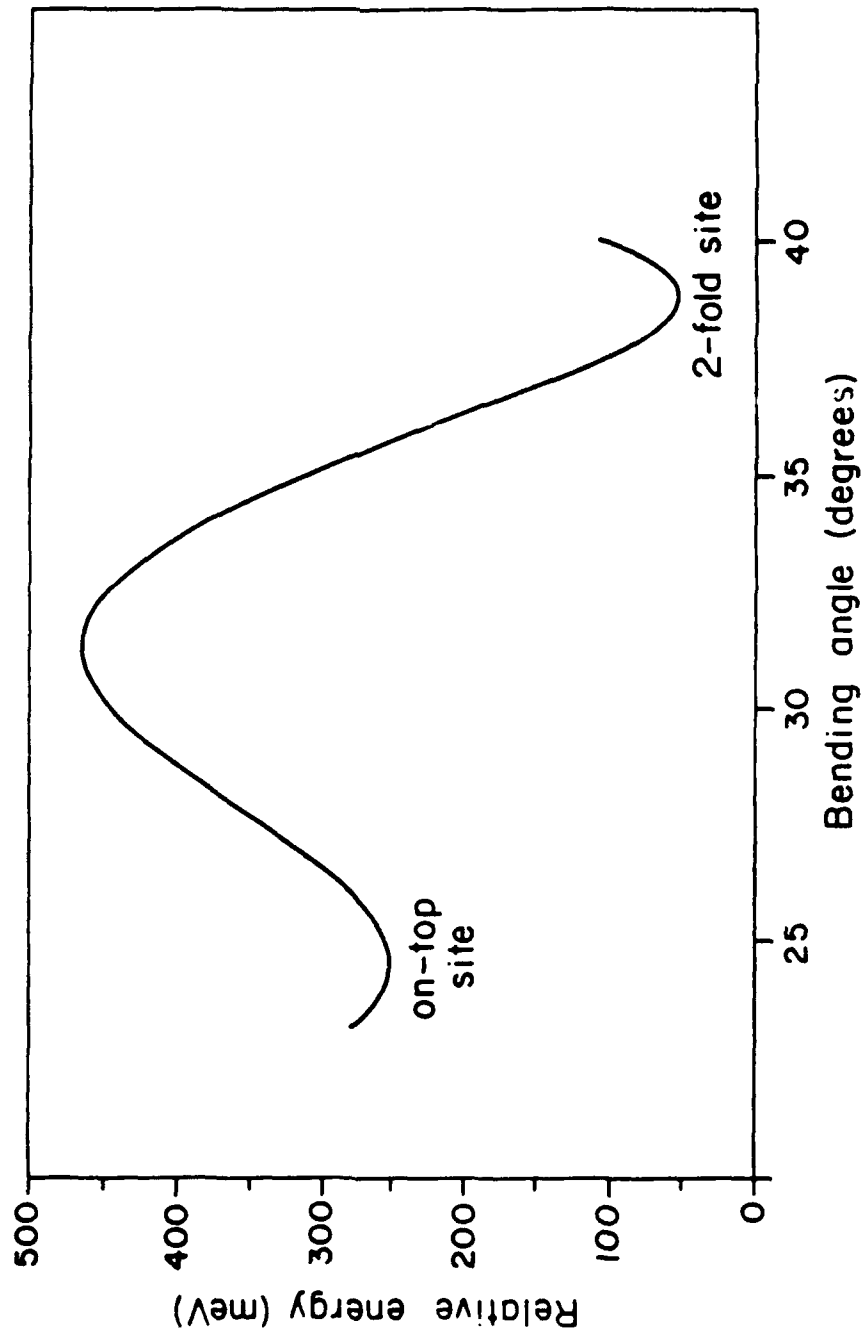


Figure 10. Energy profile for the interconversion of ethylene between Pr(2-fold) and Pr(on-top).

## Conclusion

We have investigated in detail the adsorption of ethylene on three metal surfaces, Ni(111), Pd(111) and Pt(111). Several established and useful concepts in molecular chemistry, such as the Dewar-Chatt-Duncanson model, local symmetry, three-level interactions are valuable for understanding the adsorbate-surface interaction. There are, however, some unexpected results as well. It seems that besides the d bands, the s and p bands also play a significant role in the bonding between  $\pi^*$  and the surface. Although the  $\sigma$  orbital of ethylene interacts strongly with the metal atoms, the contribution of this orbital to bonding is not significant because most of the  $\sigma$ -surface antibonding states are below the Fermi energy. In contrast, most of the  $\pi$ -surface and  $\pi^*$ -surface bonding states are occupied while their antibonding counterparts are empty. Hence, these two frontier orbitals dominate the adsorbate-surface bonding.  $\pi^*$  is the major contributor to the carbon-metal OP for Ni(2-fold), Ni(on-top), and Pt(2-fold), but  $\pi$  is more important for the other three adsorption sites. On Ni(111) and Pt(111), the  $\pi^*$ -metal bonding is much stronger at the 2-fold site than the on-top site, mainly due to level A (see scheme 11). This may be related to the slight energetic preference for Ni(2-fold) and Pt(2-fold) relative to Ni(on-top) and Pt(on-top), although at the 2-fold site there is more weakening of the C-C bond. For Pd(2-fold), most of the  $\pi^*$ -s and  $\pi^*$ -p bonding states are above the Fermi energy. As reflected by the electron occupation and the projected OP, the  $\pi^*$ -Pd interaction is only slightly strengthened on going from Pd(on-top) to Pd(2-fold). This small gain in bonding may not be enough to compensate for the C-C weakening, and thus Pd(on-top) is the more stable site.

## Appendix

Our calculations are of the tight-binding extended Hückel type with a weighted  $H_{ij}$  approximations.<sup>35,36</sup> The geometrical assumptions concerning bond lengths (in Å) include the following: C-H 1.10, C-C 1.45, Ni-C 2.02, Pd-C 2.10, Pt-C 2.10, Ni-Ni 2.49, Pd-Pd 2.75 and Pt-Pt 2.77 Å. The extended Hückel parameters are listed in Table 10. Double zeta expansions of the metal d orbitals have been employed. The parameters of ethylene are taken from previous study.<sup>37</sup> Charge iterations have been performed, assuming a quadratic dependence of metal  $H_{ii}$ 's on charge.<sup>38</sup>

The detailed procedure for obtaining the metal parameters is as follows: First we assume a bending angle of  $30^\circ$  for all six adsorption sites. We performed the charge iterations to get a set of  $H_{ij}$ 's, calling them A. We then optimized the bending angles  $\phi$ , with set A. Redoing the charge iterations with these  $\phi$ , we obtained another set of parameters, set B. Since set A was almost equal to set B,  $\phi$  remained unchanged even if we repeated the optimization of bending angles with set B. The parameters used and listed in this paper are set B.

---

Table 11 here

---

The k points are generated according to the geometrical method of Böhm and Ramirez.<sup>39</sup> Since all the six adsorption sites have the same symmetry, the same k point set (totally 18) can be and has been chosen for all calculations. In this way, the error in computing the energy difference between the on-top and 2-fold site should be minimized.

Table 11. Extended Hückel Parameters.

Atom	Orbital	$H_{ii}$ (eV)	$\zeta_1$	$\zeta_2$	$c_1$	$c_2$
C	2s	-21.4	1.62			
	2p	-11.4	1.62			
H	1s	-13.6	1.30			
Ni	4s	-7.92	2.10			
	4p	-4.18	2.10			
	3d	-11.51	5.75	2.00	0.57	0.63
Pd	5s	-7.51	2.19			
	5p	-3.86	2.15			
	4d	-12.53	5.98	2.61	0.55	0.67
Pt	6s	-8.82	2.55			
	6p	-5.28	2.55			
	5d	-12.15	6.01	2.70	0.63	0.55

## **Acknowledgements**

We offer our thanks to Professor Norman Sheppard for pointing out this interesting problem to us; his comments on our manuscript also proved invaluable. We are grateful to the Office of Naval Research for its support of this work. Acknowledgement is also made to Jane Jorgensen and Elisabeth Fields for their expert drawings.

## References

- 1 J. A. Gates and L. L. Kesmodel, *Surf. Sci.*, 1982, **120**, L461.
- 2 N. Sheppard, *Ann. Rev. Phys. Chem.*, 1988, **39**, 589.
- 3 R. Hoffmann, *Solids and Surfaces: A Chemist's View of Bonding in Extended Structures* (VCH: New York, 1988).
- 4 P. C. Stair and G. A. Somorjai, *J. Chem. Phys.*, 1977, **66**, 2036.
- 5 M. Abon, J. Billy and J. C. Bertolini, *Surf. Sci.*, 1986, **171**, L387.
- 6 S. M. Davis, F. Zaera, B. E. Gordon and G. A. Somorjai, *J. Catalysis*, 1985, **92**, 240.
- 7 N. Freyer, G. Pirug and H. P. Bonzel, *Surf. Sci.*, 1983, **125**, 327.
- 8 N. Freyer, G. Pirug and H. P. Bonzel, *Surf. Sci.*, 1983, **126**, 487.
- 9 R. Yu and T. Gustafsson, *Surf. Sci.*, 1987, **182**, L234.
- 10 R. J. Koestner, J. Stöhr, J. L. Gland and J. A. Horsley, *Chem. Phys. Lett.*, 1982, **105**, 332.
- 11 L. Hammer, T. Hertlein and K. Müller, *Surf. Sci.*, 1986, **178**, 693.
- 12 H. Steininger, H. Ibach and S. Lehwald, *Surf. Sci.*, 1982, **117**, 684.
- 13 H. Ibach and S. Lehwald, *J. Vac. Sci. Technol.*, 1978, **15**, 407.
- 14 S. Lehwald and H. Ibach, *Surf. Sci.*, 1979, **89**, 425.
- 15 L. Hammer, T. Hertlein and K. Müller, *Surf. Sci.*, 1986, **178**, 693.
- 16 T. K. Sham and R. G. Carr, *J. Chem. Phys.*, 1986, **84**, 4091.
- 17 M. B. Hugenschmidt, P. Dolle, J. Jupille and A. Cassuto, *J. Vac. Sci. Technol. A*, 1989, **7**, 3312.
- 18 (a) J. R. Anderson and C. Kemball, *Proc. R. Soc. London, Ser. A*, 1954, **223**, 361.  
(b) J. J. Rooney, F. G. Gault and C. Kemball, *Proc. Chem. Soc.*, 1960, 407.
- 19 B. F. Hegarty and J. J. Rooney, *J. Chem. Soc. Faraday Trans. 1*, 1989, **85**, 1861.
- 20 J. E. Demuth, *IBM J. Res. Dev.* 1978, **22**, 265.

- 21 J. Stöhr, F. Sette and A. L. Johnson, *Phys. Rev. Lett.*, 1984, **53**, 1684.
- 22 D. Arvanitis, L. Wenzel and K. Baberschke, *Phys. Rev. Lett.*, 1987, **59**, 2435.
- 23 D. Arvanitis, K. Baberschke, L. Wenzel and U. Döbler, *Phys. Rev. Lett.*, 1986, **57**  
3175.
- 24 J. J. Bonnet, R. Mathieu, R. Poilblanc and J. A. Ibers, *J. Am. Chem. Soc.*, 1979,  
**101**, 7487.
- 25 R. A. Love, T. F. Koetzle, G. J. B. Williams, L. C. Andrews and R. Bau,  
*Inorg. Chem.*, 1975, **14**, 2653.
- 26 G. Wilkinson, F. G. A. Stone and F. E. W. Abel, Ed., *Comprehensive Organometallic  
Chemistry*, vol 6, (Pergamon, 1982), chap 37. .8, 39
- 27 (a) D. B. Kang and A. B. Anderson, *Surf. Sci.*, 1985, **155**, 639.  
(b) A. B. Anderson, *J. Chem. Phys.*, 1976, **65**, 1729.
- 28 O. K. Andersen, *Phys. Rev. B*, 1970, **2**, 883.
- 29 M. Salmerón, G. A. Somorjai, *J. Phys. Chem.*, 1982, **86**, 341.
- 30 R. G. Windham, M. E. Bartram, B. E. Koel, *J. Phys. Chem.*, 1988, **92**, 2862.
- 31 N. Sheppard, private communication.
- 32 D. B. Poweel, J. G. V. Scott and N. Sheppard, *Spectrochim. Acta.*, 1972, **28A**, 327.
- 33 O. Eisenstein and R. Hoffmann, *J. Am. Chem. Soc.*, 1981, **103**, 4308.
- 34 K. G. Lloyd, B. Roop, A. Campion and J. M. White, *Surf. Sci.*, 1989, **214**, 227.
- 35 (a) R. Hoffmann, *J. Chem. Phys.*, 1963, **39**, 1397.  
(b) R. Hoffmann and W. N. Lipscomb, *J. Chem. Phys.*, 1962, **37**, 2872.  
(c) J. H. Ammeter, H. -B. Bürgi, J. C. Thibeault and R. Hoffmann, *J. Am. Chem.  
Soc.*, 1978, **100**, 3686.
- 36 M. -H. Whangbo and R. Hoffmann, *J. Am. Chem. Soc.*, 1978, **100**, 6093.
- 37 C. Zheng, Y. Apeloig and R. Hoffmann, *J. Am. Chem. Soc.*, 1988, **110**, 774.

- 38 S. P. McGlynn, L. G. Vanquickenborne, M. Kinoshita and D. G. Carroll, *Introduction to Applied Quantum Chemistry*, (Holt, Rinehart and Winston, Inc., 1972) pp 138-139, Appendix D.
- 39 R. Ramirez and M. C. Böhm, *Int. Quantum Chem.* 1986, **30**, 391.